Direct interaction between fd phage pilot protein pIII and the TolQ–TolR proton-dependent motor provides new insights into the import of filamentous phages

Callypso Pellegri, Ambre Moreau, Denis Duché, Laetitia Houot

Direct interaction between fd phage pilot protein pIII and the TolQ-TolR proton-dependent motor provides new insights into the import of filamentous phages

Running title: pIII interaction with TolQ and TolR

Callypso PELLEGRI, Ambre MOREAU, Denis DUCHE and Laetitia HOUOT#

Laboratoire d'Ingénierie des Systèmes Macromoléculaires, UMR7255, Institut de Microbiologie de la Méditerranée, Aix-Marseille Univ – CNRS, 31 Chemin Joseph Aiguier, CS 70071, 13402 Marseille Cedex 09, France.

Address correspondence to Dr. Laetitia Houot, lhouot@imm.cnrs.fr, tel: +33 (0)4 91 16 41 56 fax: +33 (0)4 91 71 21 24

Keywords: Filamentous bacteriophage, Tol-Pal system, infection, protein-protein interaction, proton motive force, virus entry.

ABSTRACT

Filamentous phages are one of the simplest examples of viruses with a protein capsid that protects a circular single-stranded DNA genome. The infection is very specific, non-lytic and can strongly affect the physiology or provide new pathogenic factors to its bacterial host. The infection process is proposed to rely on a pore-forming mechanism similar to that of certain non-enveloped eukaryotic viruses. The Ff coliphages (including M13, fd and f1) have been intensively studied and were used to establish the sequence of events taking place for efficient crossing of the host envelope structure. However, the mechanism involved in the penetration of the cell inner membrane is not well understood. Here, we identify new host players involved in the phage translocation mechanism. Interaction studies by a combination of in vivo biochemical methods demonstrate that the adhesion protein pIII located at the tip of the phage binds to TolQ and TolR, two proteins which form a conserved proton-dependent molecular motor in the inner membrane of the host cell. Moreover, in vivo cysteine cross-linking studies reveal that the interactions between the pIII and TolQ or TolR occur between their transmembrane helix domains and may be responding to the pmf-status of the cell. These results allow us to propose a model for the late stage of filamentous phage translocation mediated by multiple interactions with each individual component of the host TolQRA complex.

INTRODUCTION

Bacteriophages disseminate from host to host, shaping bacterial communities in all environments on Earth. Most of these viruses are equipped with molecular machineries and enzymatic domains to specifically puncture their host's envelope and inject their genome into the cell cytoplasm. Successful infection converts the host to a factory dedicated to the assembly of the phage progeny that can be finally released upon lysis of the host. Filamentous phages, however, have a unique life cycle, as they behave like symbionts, establishing a chronic infection and extruding progeny virions in the environment by secretion without killing the host. These viruses infect gram-negative bacteria by parasitising the cell envelope structures to target their host and to cross the outer membrane (OM) and the periplasm. Final uncapping of the phage particle and penetration into the inner membrane (IM) is required to complete the viral infection. However, the molecular strategy for viral genome transport from the particle to the cytoplasm is still speculative (1).

Notorious filamentous phages have been described for their ability to increase the virulence potential of their bacterial host including the sepsis and meningitis agent *Escherichia coli* O18:K1:H7, the plague bacillus *Yersinia pestis,* the meningococcal agent *Neisseria meningitidis* and the cholera agent *Vibrio cholerae* (2–5), to participate in biofilm building and resistance to environmental stresses and to improve escape from the immune system (ex: *Pseudomonas aeruginosa*) (6). Recently, filamentous phage secretion has been proven to delay healing of infected wounds, highlighting a potential interest in vaccines targeting phage particles to fight infections (7). Their potential as biocontrol agent was investigated for the crop pathogen *Erwinia* (8). Despite the intensive use of the canonical coliphage M13 (or fd) in the fields of molecular biology and phage display (9, 10), the molecular mechanisms of infection responsible for the spreading of these viruses among bacterial populations remain unclear.

The canonical coliphage particle fd is composed of 2700 copies of the major coat protein pVIII that covers the genomic circular ssDNA. Five units of the minor coat proteins cap both ends of the virus, pVII and pIX on one side, pIII and pVI on the other side (designed as the phage "head") (Fig. 1). In the producing cell, all the capsid proteins are synthesised and accumulated in the IM via transmembrane helices before being assembled into the new virions (1). A macrocomplex composed of the phage encoded-proteins pI, pIV and pXI spans the whole envelope (11) and allows assembly and secretion of the progeny virion in the environment, starting with the pVII/pIX complex, followed by an helical assembly of pVIII on the ssDNA. A precomplex of pIII/pVI finalises the structure and allows its detachment from the envelope. Recently, Conners *et al.* obtained the first cryo-EM structure for f1 nanophages, providing new insights into the organisation of both major and minor capsid proteins in the viral particle (12).

The model for filamentous phage infection involves a depolymerisation process that somehow mirrors the secretion mechanism. Two sequential bacterial receptors have been identified: the conjugative F-pilus that expands from the cell surface and TolA, the pivot protein of the Tol complex in the IM (Fig. 1A). The orchestrator of the phage import is the pIII protein located with pVI at the tip

of the phage. pIII is organised into three domains N1, N2 and C, which are separated by glycine/serine-rich linkers (Fig. 1B). Structures of pIII-N1 and pIII-N2 soluble domains have been determined (13, 14) and are not visible in the full viral structure, most likely because of the flexibility of the linkers (12). The current infection model involves a 3-step mechanism. In the reception step, the phage binds the tip of the conjugative F-pilus through the pIII-N2 domain (15). Pilus retraction has been proposed to pull the phage close to the envelope surface and possibly through the OM via the pilus secretin. This step facilitates phage infection but is not strictly required, as the F^- cells can still be infected with low efficiency (16). During the translocation step, phage crossing of the periplasmic space relies on proteins of the Tol system. Indeed, the three IM anchored proteins TolQ, TolR and TolA form a complex required for infection (17, 18). A direct interaction between the TolA globular domain (TolA3) and the phage pIII-N1 domain has been characterised by structural approaches (13, 19). The role of TolQ or TolR in the infection process is unclear. The final phage genome injection step requires opening of the phage head and insertion of the pIII C-terminal hydrophobic segment in the IM (Fig. 1A). pIII-C may assemble as a pentamer which possibly form a pore for the phage ssDNA genome to cross the IM. Indeed purified pIII proteins can form pores in artificial lipid bilayers (20). Deletion of a 28-residue-long segment in pIII-C (residues 286 to 314) strongly reduces the infectivity of the phage, while deletion of a longer segment (residues 286 to 324) renders the phage non-infective (21, 22). It has been suggested that pVI may participate in the formation of the pore (12), although this hypothesis remains to be proven experimentally. In the final step, sequential disassembly of the pVIII capsid proteins in the lipid bilayer of the host is proposed to be concomitant to viral genome transfer into the cytoplasm and to its conversion in a dsDNA replicative form (23).

The phage particle is a very robust structure and cannot be destabilised by exposure to artificial membranes or to cell membrane fractions obtained by mechanical disruption (23). Moreover, based on the predicted structure of the intact phage particle, pIII and pVI would need to undergo significant conformational changes to dive into the host membrane (12). Thus, we investigated the hypothesis that the critical step of the virion head "opening" is occurring through structural modifications driven by sequential protein-protein interactions with the host proteins. TolA, TolQ and TolR proteins form the IM complex of the Tol-Pal system, a proton motive force (pmf)-dependent molecular motor conserved in gram-negative bacteria (Fig. 1A). The TolQ-TolR motor is evolutionary related to the ExbB-ExbD motor of the Ton system, which is involved in the active transport of iron-siderophores and of cobalamin (24). TolA and TolR are both anchored to the IM via one N-terminal transmembrane helix (TMH) while TolQ is embedded via three TMHs, named Q1, Q2 and Q3. Based on biochemical analyses (25) and by homology with the ExbB-ExbD motor (26, 27), TolQ may form a pentameric structure surrounding a dimer of TolR proteins, with Q2 and Q3 interacting with TolR transmembrane helices (R1 TMH). TolR dimerises through R1 TMH into the IM and through R2 and R3 domains in the periplasm (28, 29). It has been suggested that the assembly of the TolQ-TolR motor induces conformational changes and

exposure of a peptidoglycan binding domain in TolR3 (30). In the IM, the dynamic interactions between Q2, Q3 and R1 TMHs define two proton channels which might sequentially operate. Biochemical studies, structural data and modelisation suggest that TolA TMH (TolA1) interacts with TolQ1 at the periphery of the motor (31–33). The flux of protons is converted into mechanical movements transduced to the TolA protein, which interacts with the OM lipoprotein Pal and with the periplasmic protein TolB (34–36). In *E. coli*, mutants of the Tol-Pal system display numerous defects collectively called *tol* phenotypes, such as a chaining morphology in low osmotic medium, hypersensitivity to detergents, resistance to Tol-dependent toxins called colicins (37) and increased resistance to chromate (38). Thorough analysis of these pleiotropic phenotypes over the past 50 years demonstrated that the Tol-Pal complex is crucial in envelope integrity maintenance, in OM lipid homeostasis and in the late stage of cell division (39–43).

We recently showed that phage uptake in the host required an assembled TolA-TolQ-TolR complex. Strains producing TolQ point mutants defective for pmf utilisation by the Tol system show *tol* phenotypes but remain efficient for filamentous phage import (18). We also demonstrated that the ExbB-ExbD proteins can cross-operate with TolA to drive phage import in the absence of the TolQ-TolR proteins, however without restoring the functionality of the Tol system.

In this study, we provide molecular details on the interactions occurring between the phage head protein pIII and the host inner membrane complex TolQ-TolR-TolA during infection. Bacterial two-hybrid (BACTH), co-immunoprecipitation (co-IP) experiments and a partial proteolysis assay show that the phage minor capsid protein pIII interacts with TolQ and TolR. Using shorter variants of pIII, we demonstrate that the pIII C-terminal domain is sufficient to interact with TolQ and TolR. Finally, in vivo cysteine cross-linking studies reveal that binding between the phage and the host proteins involves their TMH domains, some of the interactions responding to the pmf-status of the cell.

RESULTS

Interaction studies of the minor coat proteins constituting the fd phage head.

The phage relies on its pIII cap proteins to orchestrate targeting and penetration of the host envelope. While pIII-N1 and pIII-N2 bind to TolA3 and to the F-pilus, respectively, it is not known how pIII-C is extracted from the viral particle to insert into the IM. In the intact phage head, the five pIII C-domains are mainly organised in α-helices in close contact with five units of pVI. A pIII-C intrachain disulfide bond between Cys-354 and Cys-371 stabilises a β-hairpin upstream the hydrophobic terminal α-helix (12). The capsid proteins all have the inner membrane of the host as their final destination. We first aimed to get a better understanding of the interactions occurring between pIII, pVI, pVIII proteins and the pIII subdomains using a BACTH approach. First, the full length *g3p, g8p* and *g6p* genes of the fd phage were cloned in frame with the T18 and T25 domains of the *Bordetella pertussis* adenylate cyclase at their C-terminus. We predicted that the chimeric constructs would localise in the IM through their hydrophobic segments, with the T18 and T25 domains exposed in the cytoplasm. The assays

conducted in the BTH101 strain on reporter plates demonstrated that pIII interacts with itself as well as with pVI (Fig. 2A) as expected (44, 45). A pIII-C construct comprising residues 256 to 406, which correspond to pIII deleted of its N1 and N2 domains, was sufficient for both homo-oligomerisation and heteromerisation with pVI (Fig. 2A). Of note, our attempt to include the major coat protein pVIII to this BACTH study failed as the pVIII-T18 and pVIII-T25 fusions displayed unspecific binding to control membrane proteins (data not shown).

The sequence encoding pIII-N1 (residues 1 to 71 of the mature pIII protein), pIII-N2 (residues 82 to 222) and pIII-C deleted of its TMH ($C_{\Delta TM}$; residues 256 to 378) were fused in frame with T18 and T25 in the BACTH plasmids. As the N1 and $C_{\Delta TM}$ domains comprise two and one disulfide bonds, respectively, the Oxi-Blue strain was used to conduct the two-hybrid assay, this background derived from the Oxi-BTH strain promoting correct folding of disulfide bond structured proteins in its cytoplasm (46). As previously reported by crystallography (14) and by SPR analysis (47), we observed in the BACTH assay that pIII-N1 interacts with pIII-N2 (Fig. 2B), attesting to the correct production and folding of the constructs. pIII-N2 but not pIII-N1 was able to oligomerize. Lastly, we observed that deletion of the pIII-C TMH strongly impaired the ability of pIII-$C_{\Delta TM}$ to oligomerise despite correct production of the proteins (Fig. S1).

pIII interacts with TolR and TolQ in vivo.

Phage infection requires an assembled TolA-TolQ-TolR complex in the IM (18) although pIII-N1/TolA3 is the only direct interaction characterised in the literature (13, 17, 47). We investigated if the TolR and TolQ proteins could also act as receptors of the phage. Using the BACTH assay, we observed that pIII was able to interact with both TolR and TolQ (Fig. 3A). The interactions were confirmed by copurification and by co-immunoprecipitation (Co-IP). First, plasmids encoding TolQ with a HA-tag and pIII fused to the T18 domain were introduced by transformation into an *E. coli* W3110 strain. The membrane proteins were solubilised with a triton treatment. We purified pIII-T18 on calmodulin beads and observed by immunodetection that $TolQ_{HA}$ specifically copurified with pIII-T18 (Fig. 3B). Reciprocally, we showed that the native pIII protein specifically co-immunoprecipitated with $TolQ_{HA}$ using an anti-HA resin (Fig. 3C). Finally, TolR overproduced from a vector co-immunoprecipitated with pIII using sepharose beads customised with anti-pIII antibodies (Fig. 3D). Of note, endogenous TolR production was not sufficient to visualise the TolR-pIII co-immunoprecipitation signal. It has been previously shown that the homologous ExbB-ExbD motor can replace TolQ-TolR for phage uptake (18). In line with these data, we found that pIII is able to interact with ExbB in a BACTH assay (Fig. S2A). Altogether, our data demonstrate direct interactions between the phage pIII protein and both TolQ and TolR proteins that form the Tol motor in the inner membrane of the host. Of note, interactions between the phage protein pVI and TolQ or TolR could not be tested, as pVI stability is dependent on pIII (45). Indeed, pVI-T18 could only be immunodetected when coproduced with pIII in our assays.

pIII protects the C-terminal domain of TolQ in a proteolysis accessibility assay.

We next investigated how pIII was interacting with its partners in the bacterial membrane by performing a limited proteolytic digestion of whole cells by proteinase K. First, TolQ tagged with a C-terminal HA epitope and pIII full length proteins were co-produced from compatible expression vectors. Correct production and localisation of pIII in the membrane were attested by cell fractionation and immunodetection (Fig. S3A). The pattern of $TolQ_{HA}$ digestion by proteinase K in the absence or in the presence of pIII is shown in Figure 4. A protease-resistant $TolQ_{HA}$ fragment (referred to as $TolQ_{HA}$*) with an apparent size of 9 kDa could only be visualised when co-produced with the pIII protein. As $TolQ_{HA}$* is detected with antibodies raised against the C-terminal HA tag, this suggests that pIII protects approximately the last 80 TolQ residues from proteolysis, which correspond to the periplasmic loop and the Q3 TMH of TolQ (Fig. S2B). We also performed proteolysis experiments with TolR produced in the presence or in the absence of pIII. The resulting proteinase K digestion profile detected with a polyclonal anti-TolR antibody did not highlight any obvious protected fragment of TolR by the pIII protein. Reciprocally, the pIII proteolysis profile immunodetected with a polyclonal anti-pIII antibody did not demonstrate any specific pattern in the presence of TolQ or TolR (data not shown).

The C-terminal hydrophobic helix of pIII is required for binding to TolQ and TolR.

In order to define the segment of pIII responsible for TolQ and TolR binding, truncated versions of pIII-T18 were constructed (Fig. 5A and Fig. S1) based on the protein secondary structures (21). Our results showed that the last 132 residues of pIII-C (segment 275 to 406 of the mature protein) are sufficient for interaction with TolQ and with TolR (Fig. 5B). TolR is a membrane protein anchored by its TolR1 domain and exposing a large domain in the periplasm (TolR2-3; residue 45 to 143). We wondered if pIII and TolR were interacting via their periplasmic domains. However, we found that the soluble pIII-N1, pIII-N2 and pIII-$C_{\Delta TM}$ constructs are not able to interact with TolR2-3 in a BACTH experiment (Fig. 2B).

Periplasmic production of the soluble pIII-N1 domain (48) or full-length pIII protein production in *E. coli* cells (Fig. S3) results in increased resistance to detergent deoxycholate (DOC) and to colicin A, as well as a 4-log decrease in the sensitivity of cells to phage uptake. This has been previously suggested to result from TolA sequestration by the phage protein, an interaction involving the C-terminal domain of TolA and the pIII-N1 YGT motif (48). In accordance with this hypothesis, we observed that cells producing the $pIII_{\Delta YGT}$ protein variant showed a level of sensitivity to DOC and to the colicin A similar to the WT control cells. However, cells producing $pIII_{\Delta YGT}$ were less susceptible to fd phage infection (2 to 3-log decrease) compared to the control. Thus, $pIII_{\Delta YGT}$ still competes with phage uptake although less efficiently than the wild type pIII protein. We questioned if this competition was occurring through the C-terminal domain of pIII. Production of pIII-C from a pBAD expression vector in WT cells did not result in tol phenotypes as the cells showed normal resistance to DOC, a wild-type level of phage

infection and of sensitivity to colicin A despite correct expression and membrane localisation of the protein (Fig. S3A-D). As the pIII-C domain interacts with TolQ and TolR (Fig. 5), these data suggest that these interactions do not prevent the normal functioning of the Tol system in the cell or alternatively that the isolated pIII-C domain cannot interfere with a preassembled TolQRA complex.

In vivo disulfide bond formation identifies interfaces between pIII-C, TolR and TolQ TMHs.

The cysteine-scanning approach has been proven efficient for studying in vivo the assembly and dynamic of the TolQ-TolR-TolA TMHs in the IM (25, 29). To gain further insight into pIII multimerisation and interaction with TolQ and TolR, we introduced single cysteine mutations in the pBAD-pIII-C vector. We reasoned that thiol groups of cysteine side chains would form disulfide bonds if located at distances of 7 Å or less at the interface between interacting proteins. The selected positions (F381C, A382C and F383C) encompass a full α-helix turn at the beginning of the pIII-C membrane anchor, close to the periplasmic side of the IM. Importantly, the native pIII-C sequence also possesses two cysteine residues (C354 and C371) predicted to be engaged in an intra-molecular SS-bond and strictly required for pIII insertion into the phage particle. Whole living cells producing pIII-C wild-type or cysteine variants were treated with the oxidative agent copper (II) ortho-phenanthroline (CuOP) to promote disulfide bond formation and analysed using non-reducing SDS-PAGE conditions. Immunodetection indicated that the pIII-C variants (mature protein theoretical molecular weight (MW): 16.2 kDa) accumulated at similar levels in *E. coli* cells. The 381C, 382C and 383C substitutions promoted pIII-C homodimerisation in the presence of CuOP, while the native cysteine C354 and C371 (WT condition) did not (Fig. S4).

We then defined more precisely the organisation of the pIII-TolQ and pIII-TolR interaction interfaces based on the intermolecular cysteine cross-linking data (Fig. 6A). Cysteine mutants in the first helix turn at the periplasmic side of the TolQ1 (19C, 20C, 21C), TolQ2 (155C, 156C, 157C), TolQ3 (170C, 171C, 172C) and TolR1 (34C, 35C, 36C) TMHs have been previously described (25, 29). Analysis of some of the $TolQ_{HA}$ cysteine mutants (theoretical MW=30 kDa) under CuOP condition reveals a TolQ dimer (60 kDa) as well as an additional signal of apparent MW ~ 50 kDa (Fig. 6B). For combinations involving pIII-C 381C with TolQ 171C, pIII-C 382C with TolQ 171C and TolQ 172C, and finally pIII-C 383C with TolQ 172C, the 50 kDa signal was clearly seen by immunodetection using anti-HA (Fig. 6B) and anti-pIII antibodies (Fig. S5A). The $TolQ_{HA}$ 171C / pIII-C 382C sample was re-analysed on a separated western blot, the nitrocellulose membrane was cut in half vertically and the 50 kDa band was recognized by both the anti-HA and anti-pIII antibodies (Fig. 6C), further demonstrating that the complex includes both pIII and TolQ. In Figure S5A, heterocomplexes between pIII-C and the TolQ2 TMH were observed using anti-pIII antibodies (pIII-C 382C with TolQ 156C and TolQ 157C) (Fig. S5A), but not with anti-HA antibodies due to multiple product degradation signals (Fig. 6B). Of note, we occasionally observed that TolQ 170C formed weak heterocomplexes with pIII-C.

Interestingly, no intermolecular disulfide bond could be formed between TolQ1 and pIII-C THMs (Fig. S5B).

We performed a similar screening between pIII-C and TolR (Fig. 7A-B). Each individual TolR cysteine mutant was able to dimerise in CuOP oxidative conditions at an apparent MW of 36 kDa. pIII-C and TolR have very close molecular weights (16.2 kDa and 15.5 kDa, respectively) and tend to migrate similarly in the SDS-PAGE, which makes it difficult to discriminate homodimers from heterodimers, with the exception of the TolR 35C. A pIII-C/TolR heterocomplex was clearly detected for TolR 35C coproduced with pIII-C 381C and 383C. A faint heterodimer signal was also observed in some of our experiments with TolR 34C, 36C and pIII-C 381C, 383C. However, pIII-C 382C did not react with any of the tested positions of TolR in our assay. Overall, these data provide an initial mapping of the positioning of pIII-C, TolQ and TolR THM relative to each other in the IM, which is summarised in Figure 8A.

In order to test the importance of the interaction interfaces identified, an A382L single mutation and a F381G-F383G double mutation were introduced into the pIII-C-T18 protein. We observed that both mutants lost their ability to interact with TolQ-T25, but not with T25-TolR, in a BACTH assay (Fig. 8B). Finally, we constructed virions carrying the point mutations A382L or F381G-F383G of the pIII protein. Titer determination by spectrophotometry showed that both mutant phages were produced, albeit at a slightly lower concentration than the wild-type fd-Tc (2.5-fold decrease). Virion stability testing indicated that both mutant phages were sensitive to sarkosyl detergent, whereas WT phages were only disassembled in the presence of SDS, demonstrating that residues F381, A382 and F383 are important for the overall stability of the phage head (Fig. S6C). Interestingly, fd-Tc phages $pIII_{F381G-F383G}$ are no longer infectious, while fd-Tc virions $pIII_{A382L}$ can still infect *E. coli*, although infection efficiency is reduced by about 3 logs compared with wild-type fd-Tc phages (Fig. S6B). Thus, the stability of virions in detergents is not strictly related to their infection efficiency.

Dissipation of the pmf affects the infection process, independently of the reception step.

The energy requirement for phage uptake is still an intriguing question, as it is challenging to differentiate between the energy consumed for the reception step (ATP-dependent F-pilus assembly and retraction), the translocation step of the phage in the periplasm and the final transport of the phage DNA in the cytoplasm, coupled with ATP-dependent replication. In a previous study, we identified that TolQ T145A and T178A mutants unable to support pmf-dependent functions of the Tol-pal system were still infected by the phage, while the TolR D23A mutant was resistant (14). We decided to test the role of the pmf independently of the pilus reception step by studying phage infection in F^- cells. Indeed, cells lacking F-pilus, such as the W3110 strain, can be infected by filamentous phages when treated with $CaCl_2$ (16). Carbonyl cyanide m-chlorophenylhydrazone (CCCP) can bind and transport protons across the cell IM, making it a powerful uncoupler even for short, low-concentration exposure (35). W3110 F^- cells were pre-incubated with 10 µM CCCP for 3 min to dissipate the pmf then, the protonophore was

removed before phage addition in 50 mM $CaCl_2$ buffer. After incubation, cells were subject to two rounds of vortex and washes to remove free phages and reversibly adherent phages. Then, cells were incubated in LB for 10 min for metabolism recovery before enumeration of the infected cells on tetracycline supplemented LB plates. In this assay, we observed that the CCCP treated cells were 200-fold less susceptible to phage infection than the control experiment while the treatment had no impact on cell survival (Table S1).

The pmf status of the cell influence pIII hetero-dimerisation with TolQ but not with TolR.

As the TolQ-TolR motor is powered by the pmf, we wondered the interaction interfaces between pIII, TolQ and TolR TMHs were linked to the energy status of the system. For the cysteine positions that displayed the most reproducible TolR/pIII-C and TolQ/pIII-C heterodimer signals, the cells were treated with the protonophore CCCP prior to the CuOP treatment. Interactions were monitored by in vivo disulfide bond formation and immunodetection (Fig. 6D and 7). Abolition of the cell pmf had no effect on the formation of the pIII-C/TolR heterocomplexes in the IM (Figure 7). However, we observed that the formation of some pIII-C/TolQ heterodimers was strongly affected and even abolished in the absence of pmf (pIII-C 382C/TolQ 171C; pIII-C 382C/TolQ 156C; pIII-C 382C/TolQ 157C) while others were moderately affected or unaffected (pIII-C 382C/TolQ 172C; pIII-C 383C/TolQ 172C) (Fig. 6D). Interestingly, we occasionally observed (about 50% of our blots) that homodimerisation of pIII-C 382C was also dependent on the pmf, while that of pIII-C 381C and pIII-C 383C were not (Fig. 6D, right panel). Altogether, these data suggest that the pIII TMH responds to the pmf to adopt a specific position relative to TolQ, but not to TolR (Fig. 8). The pIII TMH (VFAFLLYVATFMYVFSTFANIL) is mainly composed of hydrophobic residues, with the exception of the polar residues T389, S395, T396 and N399 that could be relevant for functional or structural roles. Indeed, in the TolQ-TolR complex, highly conserved threonine residues within the TolQ2 (T145) and TolQ3 (T178) TMHs are proposed to stabilise the protonation of TolR D23, similarly to what is observed in the homologous ExbB-ExbD and MotA-MotB motors (27, 49, 50). To investigate this hypothesis, we compared the fd pIII-C TM sequence to other filamentous phage adhesion proteins that have been reported to bind to TolA in the literature, namely the coliphages If1 and IKe and the vibriophage CTX. Alignment of their C-terminal TM helices highlights a global conservation of the polar positions for the coliphages, but not the vibriophage (Fig. S6A). We constructed fd phages carrying single or double mutations at these positions of interest (T389A-T396A; S395A; N399A) and determined that the phage variants produced were as infectious as the WT virus (Fig. S6B). Thus, none of the polar residues of the C-terminal hydrophobic helix of pIII is strictly required for successful infection.

DISCUSSION

Filamentous phages are often mistakenly considered as simplistic viruses, as their genome is "simply" covered by a helical assembly of major coat proteins forming a flexible capsid which ends

with a couple of minor coat proteins at both extremities. However, these particles are highly resistant to harsh environments and do not disassemble easily. For the past 10 years, the mechanistic model of phage translocation across the bacterial periplasm during infection has evolved little, conserving black boxes in the process. Bennet *et al.* previously identified that the unlocking of the fd virion in the final step of infection is mediated by the C domain of pIII (21). More precisely, the C2 α-helix in pIII-C is essential for both infection and phage stability, as it folds over the hydrophobic pVI protein in the phage head and thus isolates it from the hydrophilic environment. This helix is comprised of the 28-long sequence required for efficient infection and previously referred to as the Infection Competence Segment (ICS Fig. 5A) It has been suggested that the phage head transitions between a closed, stable state and an open state allowing the C-terminal hydrophobic helices of pVI and pIII to insert into the membrane. This opening would require the active displacement of the C2 α-helix, possibly through a twist at the L4 linker (12). However, this hypothesis does not explain why phages deleted from the C2 domain, and thus in an "open" state, are less infectious than the WT phages (12). In this study, we formally demonstrate that pIII directly interacts with both the TolQ and the TolR proteins in vivo by BACTH and co-immunoprecipitation assays. A truncated pIII-C domain comprising residues 275 to 406 of the protein is required for interaction with TolQ and with TolR in a BACTH assay. Conversely, shorter versions of pIII-C (residues 286 to 406), and therefore lacking the entire C2 helix, cannot interact with TolQ (Fig. 5). These results suggest that C2 might be directly or indirectly involved in pIII-C interaction with TolQ (but not TolR) and provide an explanation for its requirement for efficient infection (12). Finally, we observed that pIII protects the approximate 80 terminal residues of TolQ from proteolysis, which correspond to the periplasmic loop and the TMH3 of TolQ (Fig. S2B). As proteinase K digests proteins preferentially after hydrophobic or aromatic residues, we believe that TolQ Ala162 or Leu164 might be masked by pIII binding and that the periplasmic portion of TolQ might bind to pIII. Alphafold modelisation of the pIII-C/TolQ complex indeed position the L164 and A162 residues at the interface between the two partners, the pIII ß-hairpin loop burying part of the TolQ loop in the structure (Fig. S7A-B). Interestingly, the L164 residue is one of the most conserved positions in the TolQ and ExbB periplasmic loops (Fig. S2B). Overall, TolQ and ExbB share 65.3% identity and 77.5% similarity on the TMH2-loop-THM3 sequence, which could explain why ExbB can interact with pIII-C (Fig. S2A) and supports phage import in the absence of TolQR (18). Furthermore, the conservation of the TolQ TMH2-loop-TMH3 sequence and TolR TMH in *V. cholerae* (100% identity on the transmembrane domains, 83.33% identity on the loop segment; Fig. S2B) and of TolR THM may also explain why a hybrid coliphage composed of the CTXΦ pIII N1-N2 domains fused to the FfΦ pIII-C domain is infectious to *V. cholerae* (51).

This pattern is reminiscent of the translocation determinants identified for several colicins, which are bacterial toxins that rely on a subset of the Tol proteins for uptake (52). For example, Colicin N, Colicin A and Colicin K are pore-forming toxins that require TolA, TolQ, TolR (and TolB for ColA and ColK) for translocation. Colicin K was found to bind to TolA, TolQ and TolR independently (53).

To determine how pIII, TolR and TolQ interact in the IM, we performed a cysteine scanning of pIII and provided a first mapping of the organisation of the transmembrane helices relative to each other. First, the interaction signals between pIII and TolQ THM define a heterodimerisation interface involving Q2 (156, 157) and Q3 (171, 172), but not Q1. Interestingly, in the TolQ-TolR motor, Q2, Q3 and TolR TMHs delimit the channel by which the ions transit. Q2 and Q3 are oriented towards the centre of the complex and the dimer of TolR, while Q1 is at the periphery where it interacts with the transmembrane anchor of TolA (31, 32). We show here that the pIII-TolQ and the pIII-TolR interactions can be observed independently. One important question that remains to be addressed is to determine if pIII-C interacts simultaneously or sequentially with TolQ and TolR. To date, complex structure predictions using Alphafold does not fully fit our cysteine cross-linking data (Fig. S7C-E). This in silico approach did not allow us to model a complex including the three proteins, since pIII-C was excluded from the TolQ-TolR heterodimer in the prediction (Fig. S7F-G).

The other intriguing question is the role played by TolQ and TolR when the phage reaches the IM. A possibility is that contact with the TolQR complex triggers the extraction of the pIII C-terminal helix and its positioning into the IM. TolQ-TolR form the proton-dependent motor required for TolA mechanical movement in the periplasm. According to our data, pIII-C does not position itself at the periphery of the motor against Q1, as is the case with TolA. Thus, our work supports the idea that pIII does not mimic TolA to harvest the energy from the TolQ-TolR complex to trigger phage head opening. These findings are also consistent with our previous work demonstrating that strains producing assembled but non-functional motors (TolQ T145A and TolQ T178A variants) are still susceptible to phage infection (18). In contrast, the identified interactions suggest that the phage protein pIII mobilises TolQ and TolR TMHs in a specific arrangement distinct from the TolQRA 5:2:1 complex. The interaction between the phage and TolA could be the first step in the process, transmitting long-distance structural rearrangements in TolQR, in pIII-C or in both partners. One possibility is that pIII-C induces disassembly of the TolQ-TolR motor complex or the displacement of one or several units of TolQ or TolR from the TolQR complex. This would trigger the extraction of the hydrophobic helix of pIII-C from the particle and its burial in the IM. Alternatively, pIII-C could mobilise free TolQ and TolR proteins not engaged into the motor complexes. However, the fact that infection relies on the existence of assembled Q-R-A complexes (18) does not support the latter hypothesis. There is currently no information on the nature of the pore allowing the phage to transfer its DNA through the IM, although it probably comprises a pentamer of pIII and possibly of pVI. The TMH of TolQ and/or TolR might also be part of the pore. To date, it is challenging to reconcile the results and the faces of TM segments in interaction in the TolQR complex. The fact that pIII-C homodimers and heterodimers with TolR do not point out a defined interface suggests that movements of helices in the IM may occur, as it is the case for TolR homodimers (29). However, we observed that residues A382 and F381/F383 are important for pIII-TolQ interaction (Fig. 8B) and probably for the structuring of the phage head (Fig. S6C), these data being consistent with their position in the virion structure recently solved (PBD:8B3O) (12). The

mechanism by which pIII-TolQ interaction responds to the pmf (see Fig. 6D) remains to be determined. The recent breakthrough in the experimental resolution of the homologous ExbB-ExbD complex structure by cryoEM may now serve the study of pIII-C interaction with TolQR (26).

In conclusion, our studies suggest a novel host-assisted step in the molecular process used by filamentous phages for gaining entry into bacteria. The adhesion protein pIII confirms here its role as a pilot involved in each step of the translocation process, from the extracellular environment to the cell IM, through its organisation in distinct specialised subdomains. These findings will help to understand the structural basis for filamentous phage Tol-mediated membrane penetration mechanisms in a broad range of biomedically important bacterial pathogens.

EXPERIMENTAL PROCEDURES

Bacterial strains, medium and growth conditions.

Bacterial strains and plasmids used in this study are listed in Supplemental Table S2. Bacteria were routinely cultivated in Luria-Bertani broth (LB) at 37°C with agitation at 160 rpm. When indicated, antibiotics were added to the medium at the following concentrations: ampicillin (50 or 100 µg/ml), kanamycin (50 µg/ml) and tetracycline (15 µg/ml).

Plasmid construction

Sequence amplifications by Polymerase Chain Reactions (PCR) were performed using Q5 High Fidelity DNA polymerase (NEB) and pairs of primers (Sigma Aldrich) listed in Table S2. Plasmids were constructed using standard cloning techniques, as previously described (18, 25). Point mutants on expression plasmids were obtained by Quick-change site-directed mutagenesis using complementary pairs of oligonucleotides (Table S2) and Pfu Turbo polymerase (Agilent). All constructs were confirmed by DNA sequencing (Eurofins, MWG).

Protein-protein interaction assays

Bacterial Two-Hybrid Assay in E. coli BTH101 and Oxi-Blue strains— The Oxi-Blue strain used for two-hybrid experiments is a *lac*+ derivative of the Oxi-BTH strain previously engineered to study interactions between proteins with disulfide bonds (46). Briefly, the Oxi-BTH strain (*lacZ*⁻) is deleted for glutaredoxin reductase (*gor*) and thioredoxin reductase (*trxB*) genes, which allows disulfide bond formation in the cytoplasm, while cytoplasmic expression of the isomerase DsbC promotes correct disulfide bond formation for proteins containing more than two cysteines. The *lacZ* gene was transduced in this background using a P1-lysate of an *E. coli* K12 lacZ+ strain (Gift from Dr. E. Bouveret). The resulting strain, named Oxi-Blue, can be screened on either X-Gal or MacConkey plates. Interaction experiments by the bacterial adenylate cyclase-based two-hybrid technique (BACTH) were conducted

as previously published (46). The experiments were done at least in triplicate and a representative assay is shown.

Protein modelling.

Alphafold2 and Alphafold multimer webserver interfaces (54) were used to model the protein structures. The available structures of pIII-N1 (pdb:1TOL) and pIII-N1-N2 (pdb:1G3) were retrieved from the Protein Data Base. Visual representations of the structures were prepared with ChimeraX (55).

In vivo disulfide bond formation and immunodetection.

Cysteine scanning was carried out as previously described (29) with slight modifications. $8x10^8$ exponentially growing W3110 cells were harvested and resuspended in 1 ml of 20 mM sodium phosphate buffer (PBS, pH 6.8) and then treated for 10 min with 2.5 mM N-ethylmaleimide (NEM; Sigma) to block reduced thiol groups. When required, cells were treated with the oxidative catalyst copper (II) orthophenanthroline 0.3 mM (CuOP; Sigma) for 15 min prior washing in sodium phosphate buffer and blocking with NEM for 20 min. After centrifugation, cell pellets were resuspended in Laemmli loading buffer in absence of the reducing agent. For disulfide bond formation experiments in energy depletion conditions, cells were first treated with 40 µM carbonyl cyanide m-chlorophenylhydrazone (CCCP; Sigma) for 15 min prior to CuOP labelling.

Coimmunoprecipitation.

Coimmunoprecipitation experiments were performed as previously described (53). Exponentially growing cells ($2x10^9$) were collected, washed with 20 ml of 10 mM sodium phosphate buffer (NaPi pH 6.8) and resuspended in NaPi buffer supplemented with 1% formaldehyde. Cells were incubated at room temperature for 20 min, the cross-linking reaction was stopped by the addition of 0.3 M Tris-HCl (pH 6.8) and the cells were finally washed in 20 mM Tris-HCl (pH 6.8). The membrane proteins were solubilised for 30 min at 37°C in TES (10 mM Tris-HCl, pH 7.5, 5 mM EDTA, 1% SDS) in the presence of protease inhibitors (Complete; Roche) and diluted 15-fold in TNE (10 mM Tris-HCl, pH 7.5, 5 mM EDTA, 150 mM NaCl) supplemented with 1% Triton X-100. After incubation for 2 h at room temperature with vigorous shaking, the extract was centrifuged for 30 min at 14,000 g to remove unsolubilized material. One mL of each supernatants was then incubated overnight at 4°C with anti-HA agarose beads (Cell Signaling Technology #3956S) or Protein-A sepharose CL-4B beads (GE Healthcare) customised with 2 µl antibodies against pIII (Mobitech). Beads were then washed twice with TNE supplemented with 1% Triton X-100, once in TNE supplemented with 0.1% Triton X-100 and 0.1% Tween, and once in TNE supplemented with 0.1% TritonX-100. The immunoprecipitated material was heated in loading buffer prior to analyses by SDS-PAGE and immunoblotting.

SDS-PAGE and Immunoblotting

Protein samples resuspended in 2x loading buffer (Tris-HCl 100 mM pH 6.8, SDS 2%, glyceerol 10%, bromophenol blue 0.01%, 5% 2-β-mercaptoethanol) were subjected to sodium dodecyl sulphate (SDS)-polyacrylamide gel electrophoresis (PAGE). For detection by immunostaining, proteins were transferred onto nitrocellulose membranes, and immunoblots were probed with primary antibodies followed by goat secondary antibodies coupled to alkaline phosphatase and developed in alkaline buffer in presence of 5-bromo-4-chloro-3-indolylphosphate (BCIP) and nitroblue tetrazolium (NBT). The anti-TolA3 and anti-TolR polyclonal antibodies are from our laboratory collection while the anti-pIII monoclonal antibody (NEB), the anti-HA monoclonal antibody (Invitogen) and alkaline phosphatase-conjugated goat anti-rabbit and anti-mouse antibodies (Millipore) have been purchased as indicated.

Data availability

All data for this work are contained in this manuscript.

Supporting information

This article contains supporting information.

Acknowledgements— *We thank the members of the Cascales, Roussel, Durand and Sturgis research groups for numerous discussions and technical advices, and Christophe Bernard and Roland Lloubès for insightful comments on the manuscript. We thank Rachida Es-Smimih for plasmid constructions and Emmanuelle Bouveret (Pasteur Institute) for sharing some BACTH vectors with us. We are grateful to the LISM technical staff for assistance in media preparation and to Burt Hatartynn for encouragements. We acknowledge UCSF ChimeraX for molecular graphics. CP is supported by a PhD fellowship from Aix-Marseille Univ. Work in the laboratory is supported by the Centre National de la Recherche Scientifique (CNRS), the Aix-Marseille Univ. and by Agence Nationale de la Recherche (ANR-18-CE11-0027).*

Conflict of interest—The authors declare that they have no conflicts of interest with the contents of this article.

References

1. Hay, I. D., and Lithgow, T. (2019) Filamentous phages: masters of a microbial sharing economy. *EMBO Rep*. 10.15252/embr.201847427
2. Bille, E., Meyer, J., Jamet, A., Euphrasie, D., Barnier, J.-P., Brissac, T., Larsen, A., Pelissier, P., and Nassif, X. (2017) A virulence-associated filamentous bacteriophage of Neisseria meningitidis increases host-cell colonisation. *PLoS Pathog*. **13**, e1006495
3. Derbise, A., Chenal-Francisque, V., Pouillot, F., Fayolle, C., Prévost, M., Médigue, C., Hinnebusch, B. J., and Carniel, E. (2007) A horizontally acquired filamentous phage contributes to the pathogenicity of the plague bacillus. *Molecular Microbiology*. **63**, 1145–1157

4. Gonzalez, M. D., Lichtensteiger, C. A., Caughlan, R., and Vimr, E. R. (2002) Conserved Filamentous Prophage in *Escherichia coli* O18:K1:H7 and *Yersinia pestis* Biovar orientalis. *J Bacteriol*. **184**, 6050–6055
5. Waldor, M. K., and Mekalanos, J. J. (1996) Lysogenic Conversion by a Filamentous Phage Encoding Cholera Toxin. *Science*. **272**, 1910–1914
6. Sweere, J. M., Van Belleghem, J. D., Ishak, H., Bach, M. S., Popescu, M., Sunkari, V., Kaber, G., Manasherob, R., Suh, G. A., Cao, X., de Vries, C. R., Lam, D. N., Marshall, P. L., Birukova, M., Katznelson, E., Lazzareschi, D. V., Balaji, S., Keswani, S. G., Hawn, T. R., Secor, P. R., and Bollyky, P. L. (2019) Bacteriophage trigger antiviral immunity and prevent clearance of bacterial infection. *Science*. **363**, eaat9691
7. Bach, M. S., de Vries, C. R., Khosravi, A., Sweere, J. M., Popescu, M. C., Chen, Q., Demirdjian, S., Hargil, A., Van Belleghem, J. D., Kaber, G., Hajfathalian, M., Burgener, E. B., Liu, D., Tran, Q.-L., Dharmaraj, T., Birukova, M., Sunkari, V., Balaji, S., Ghosh, N., Mathew-Steiner, S. S., El Masry, M. S., Keswani, S. G., Banaei, N., Nedelec, L., Sen, C. K., Chandra, V., Secor, P. R., Suh, G. A., and Bollyky, P. L. (2022) Filamentous bacteriophage delays healing of Pseudomonas-infected wounds. *Cell Reports Medicine*. **3**, 100656
8. Akremi, I., Holtappels, D., Brabra, W., Jlidi, M., Hadj Ibrahim, A., Ben Ali, M., Fortuna, K., Ahmed, M., Meerbeek, B. V., Rhouma, A., Lavigne, R., Ben Ali, M., and Wagemans, J. (2020) First Report of Filamentous Phages Isolated from Tunisian Orchards to Control Erwinia amylovora. *Microorganisms*. **8**, 1762
9. Rakonjac, J., Bennett, N. J., Spagnuolo, J., Gagic, D., and Russel, M. (2011) Filamentous bacteriophage: biology, phage display and nanotechnology applications. *Curr Issues Mol Biol*. **13**, 51–76
10. Henry, K. A., Arbabi-Ghahroudi, M., and Scott, J. K. (2015) Beyond phage display: non-traditional applications of the filamentous bacteriophage as a vaccine carrier, therapeutic biologic, and bioconjugation scaffold. *Front. Microbiol.* 10.3389/fmicb.2015.00755
11. Conners, R., McLaren, M., Łapińska, U., Sanders, K., Stone, M. R. L., Blaskovich, M. A. T., Pagliara, S., Daum, B., Rakonjac, J., and Gold, V. A. M. (2021) CryoEM structure of the outer membrane secretin channel pIV from the f1 filamentous bacteriophage. *Nat Commun*. **12**, 6316
12. Conners, R., León-Quezada, R. I., McLaren, M., Bennett, N. J., Daum, B., Rakonjac, J., and Gold, V. A. M. (2023) Cryo-electron microscopy of the f1 filamentous phage reveals insights into viral infection and assembly. *Nat Commun*. **14**, 2724
13. Lubkowski, J., Hennecke, F., Plückthun, A., and Wlodawer, A. (1999) Filamentous phage infection: crystal structure of g3p in complex with its coreceptor, the C-terminal domain of TolA. *Structure*. **7**, 711–722
14. Lubkowski, J., Hennecke, F., Plückthun, A., and Wlodawer, A. (1998) The structural basis of phage display elucidated by the crystal structure of the N-terminal domains of g3p. *Nat Struct Mol Biol*. **5**, 140–147
15. Caro, L. G., and Schnös, M. (1966) The attachment of the male-specific bacteriophage F1 to sensitive strains of Escherichia coli. *Proc Natl Acad Sci U S A*. **56**, 126–132
16. Russel, M., Whirlow, H., Sun, T. P., and Webster, R. E. (1988) Low-frequency infection of F- bacteria by transducing particles of filamentous bacteriophages. *J Bacteriol*. **170**, 5312–5316
17. Riechmann, L., and Holliger, P. (1997) The C-Terminal Domain of TolA Is the Coreceptor for Filamentous Phage Infection of E. coli. *Cell*. **90**, 351–360
18. Samire, P., Serrano, B., Duché, D., Lemarié, E., Lloubès, R., and Houot, L. (2020) Decoupling Filamentous Phage Uptake and Energy of the TolQRA Motor in Escherichia coli. *J Bacteriol*. 10.1128/JB.00428-19
19. Deprez, C., Lloubès, R., Gavioli, M., Marion, D., Guerlesquin, F., and Blanchard, L.

(2005) Solution Structure of the E.coli TolA C-terminal Domain Reveals Conformational Changes upon Binding to the Phage g3p N-terminal Domain. *Journal of Molecular Biology*. **346**, 1047–1057
20. Glaser-Wuttke, G., Keppner, J., and Rasched, I. (1989) Pore-forming properties of the adsorption protein of filamentous phage fd. *Biochimica et Biophysica Acta (BBA) - Biomembranes*. **985**, 239–247
21. Bennett, N. J., Gagic, D., Sutherland-Smith, A. J., and Rakonjac, J. (2011) Characterization of a Dual-Function Domain That Mediates Membrane Insertion and Excision of Ff Filamentous Bacteriophage. *Journal of Molecular Biology*. **411**, 972–985
22. Bennett, N. J., and Rakonjac, J. (2006) Unlocking of the Filamentous Bacteriophage Virion During Infection is Mediated by the C Domain of pIII. *Journal of Molecular Biology*. **356**, 266–273
23. Marco, R., Jazwinski, S. M., and Kornberg, A. (1974) Binding, eclipse, and penetration of the filamentous bacteriophage M13 in intact and disrupted cells. *Virology*. **62**, 209–223
24. Ratliff, A. C., Buchanan, S. K., and Celia, H. (2022) The Ton Motor. *Front Microbiol*. **13**, 852955
25. Zhang, X. Y.-Z., Goemaere, E. L., Seddiki, N., Célia, H., Gavioli, M., Cascales, E., and Lloubes, R. (2011) Mapping the Interactions between Escherichia coli TolQ Transmembrane Segments. *Journal of Biological Chemistry*. **286**, 11756–11764
26. Celia, H., Botos, I., Ni, X., Fox, T., De Val, N., Lloubes, R., Jiang, J., and Buchanan, S. K. (2019) Cryo-EM structure of the bacterial Ton motor subcomplex ExbB–ExbD provides information on structure and stoichiometry. *Commun Biol*. **2**, 358
27. Celia, H., Noinaj, N., Zakharov, S. D., Bordignon, E., Botos, I., Santamaria, M., Barnard, T. J., Cramer, W. A., Lloubes, R., and Buchanan, S. K. (2016) Structural insight into the role of the Ton complex in energy transduction. *Nature*. **538**, 60–65
28. Journet, L., Rigal, A., Lazdunski, C., and Bénédetti, H. (1999) Role of TolR N-Terminal, Central, and C-Terminal Domains in Dimerization and Interaction with TolA and TolQ. *J Bacteriol*. **181**, 4476–4484
29. Zhang, X. Y.-Z., Goemaere, E. L., Thomé, R., Gavioli, M., Cascales, E., and Lloubés, R. (2009) Mapping the Interactions between Escherichia coli Tol Subunits. *Journal of Biological Chemistry*. **284**, 4275–4282
30. Wojdyla, J. A., Cutts, E., Kaminska, R., Papadakos, G., Hopper, J. T. S., Stansfeld, P. J., Staunton, D., Robinson, C. V., and Kleanthous, C. (2015) Structure and Function of the Escherichia coli Tol-Pal Stator Protein TolR. *Journal of Biological Chemistry*. **290**, 26675–26687
31. Webby, M. N., Williams-Jones, D. P., Press, C., and Kleanthous, C. (2022) Force-Generation by the Trans-Envelope Tol-Pal System. *Front. Microbiol.* **13**, 852176
32. Germon, P., Ray, M.-C., Vianney, A., and Lazzaroni, J. C. (2001) Energy-Dependent Conformational Change in the TolA Protein of *Escherichia coli* Involves Its N-Terminal Domain, TolQ, and TolR. *J Bacteriol*. **183**, 4110–4114
33. Germon, P., Clavel, T., Vianney, A., Portalier, R., and Lazzaroni, J. C. (1998) Mutational Analysis of the *Escherichia coli* K-12 TolA N-Terminal Region and Characterization of Its TolQ-Interacting Domain by Genetic Suppression. *J Bacteriol*. **180**, 6433–6439
34. Bonsor, D. A., Hecht, O., Vankemmelbeke, M., Sharma, A., Krachler, A. M., Housden, N. G., Lilly, K. J., James, R., Moore, G. R., and Kleanthous, C. (2009) Allosteric β-propeller signalling in TolB and its manipulation by translocating colicins. *EMBO J*. **28**, 2846–2857
35. Cascales, E., Gavioli, M., Sturgis, J. N., and Lloubes, R. (2000) Proton motive force

drives the interaction of the inner membrane TolA and outer membrane Pal proteins in Escherichia coli. *Mol Microbiol*. **38**, 904–915
36. Walburger, A., Lazdunski, C., and Corda, Y. (2002) The Tol/Pal system function requires an interaction between the C-terminal domain of TolA and the N-terminal domain of TolB: Tol/Pal system function needs ToA/TolB interaction. *Molecular Microbiology*. **44**, 695–708
37. Lloubès, R., Cascales, E., Walburger, A., Bouveret, E., Lazdunski, C., Bernadac, A., and Journet, L. (2001) The Tol-Pal proteins of the Escherichia coli cell envelope: an energized system required for outer membrane integrity? *Research in Microbiology*. **152**, 523–529
38. Chaouche, A. A., Houot, L., Duché, D., Iobbi-Nivol, C., Giudici-Orticoni, M.-T., Fons, M., and Méjean, V. (2022) The Tol-Pal system of Escherichia coli plays an unexpected role in the import of the oxyanions chromate and phosphate. *Research in Microbiology*. 10.1016/j.resmic.2022.103967
39. Baccelli, P., Rachedi, R., Serrano, B., Petiti, M., Bernard, C. S., Houot, L., and Duche, D. (2022) Timing of TolA and TolQ Recruitment at the Septum Depends on the Functionality of the Tol-Pal System. *Journal of Molecular Biology*. **434**, 167519
40. Gerding, M. A., Ogata, Y., Pecora, N. D., Niki, H., and De Boer, P. A. J. (2007) The *trans* -envelope Tol–Pal complex is part of the cell division machinery and required for proper outer-membrane invagination during cell constriction in *E. coli*. *Molecular Microbiology*. **63**, 1008–1025
41. Gray, A. N., Egan, A. J., van't Veer, I. L., Verheul, J., Colavin, A., Koumoutsi, A., Biboy, J., Altelaar, A. F. M., Damen, M. J., Huang, K. C., Simorre, J.-P., Breukink, E., den Blaauwen, T., Typas, A., Gross, C. A., and Vollmer, W. (2015) Coordination of peptidoglycan synthesis and outer membrane constriction during Escherichia coli cell division. *eLife*. **4**, e07118
42. Petiti, M., Serrano, B., Faure, L., Lloubes, R., Mignot, T., and Duché, D. (2019) Tol Energy-Driven Localization of Pal and Anchoring to the Peptidoglycan Promote Outer-Membrane Constriction. *Journal of Molecular Biology*. **431**, 3275–3288
43. Shrivastava, R., Jiang, X., and Chng, S.-S. (2017) Outer membrane lipid homeostasis via retrograde phospholipid transport in *Escherichia coli*: A physiological function for the Tol-Pal complex. *Molecular Microbiology*. **106**, 395–408
44. Gailus, V., and Rasched, I. (1994) The adsorption protein of bacteriophage fd and its neighbour minor coat protein build a structural entity. *Eur J Biochem*. **222**, 927–931
45. Rakonjac, J., and Model, P. (1998) Roles of pIII in filamentous phage assembly. *Journal of Molecular Biology*. **282**, 25–41
46. Houot, L., Navarro, R., Nouailler, M., Duché, D., Guerlesquin, F., and Lloubes, R. (2017) Electrostatic interactions between the CTX phage minor coat protein and the bacterial host receptor TolA drive the pathogenic conversion of Vibrio cholerae. *Journal of Biological Chemistry*. **292**, 13584–13598
47. Karlsson, F., Borrebaeck, C. A. K., Nilsson, N., and Malmborg-Hager, A.-C. (2003) The Mechanism of Bacterial Infection by Filamentous Phages Involves Molecular Interactions between TolA and Phage Protein 3 Domains. *J Bacteriol*. **185**, 2628–2634
48. Pommier, S., Gavioli, M., Cascales, E., and Lloubès, R. (2005) Tol-dependent macromolecule import through the Escherichia coli cell envelope requires the presence of an exposed TolA binding motif. *J Bacteriol*. **187**, 7526–7534
49. Deme, J. C., Johnson, S., Vickery, O., Aron, A., Monkhouse, H., Griffiths, T., James, R. H., Berks, B. C., Coulton, J. W., Stansfeld, P. J., and Lea, S. M. (2020) Structures of the stator complex that drives rotation of the bacterial flagellum. *Nat Microbiol*. **5**, 1553–1564
50. Goemaere, E. L., Devert, A., Lloubès, R., and Cascales, E. (2007) Movements of the

TolR C-terminal domain depend on TolQR ionizable key residues and regulate activity of the Tol complex. *J Biol Chem*. **282**, 17749–17757
51. Heilpern, A. J., and Waldor, M. K. (2003) pIII ^{CTX} , a Predicted CTXφ Minor Coat Protein, Can Expand the Host Range of Coliphage fd To Include *Vibrio cholerae*. *J Bacteriol*. **185**, 1037–1044
52. Duché, D., and Houot, L. (2019) Similarities and Differences between Colicin and Filamentous Phage Uptake by Bacterial Cells. *EcoSal Plus*. **8**, ecosalplus.ESP-0030-2018
53. Barnéoud-Arnoulet, A., Gavioli, M., Lloubès, R., and Cascales, E. (2010) Interaction of the Colicin K Bactericidal Toxin with Components of Its Import Machinery in the Periplasm of *Escherichia coli*. *J Bacteriol*. **192**, 5934–5942
54. Jumper, J., Evans, R., Pritzel, A., Green, T., Figurnov, M., Ronneberger, O., Tunyasuvunakool, K., Bates, R., Žídek, A., Potapenko, A., Bridgland, A., Meyer, C., Kohl, S. A. A., Ballard, A. J., Cowie, A., Romera-Paredes, B., Nikolov, S., Jain, R., Adler, J., Back, T., Petersen, S., Reiman, D., Clancy, E., Zielinski, M., Steinegger, M., Pacholska, M., Berghammer, T., Bodenstein, S., Silver, D., Vinyals, O., Senior, A. W., Kavukcuoglu, K., Kohli, P., and Hassabis, D. (2021) Highly accurate protein structure prediction with AlphaFold. *Nature*. **596**, 583–589
55. Pettersen, E. F., Goddard, T. D., Huang, C. C., Meng, E. C., Couch, G. S., Croll, T. I., Morris, J. H., and Ferrin, T. E. (2021) UCSF CHIMERAX : Structure visualization for researchers, educators, and developers. *Protein Science*. **30**, 70–82

Figure legends

FIGURE 1. **Schematic representation of the phage import process.** A. The TolA-dependent translocation step (left) and the final phage disassembly in the inner membrane (right) are presented, highlighting the localisations and suggested topologies of the proteins of interest. The different protein domains are presented according to previously published literature. The phage head is composed of five copies of pIII and pVI, only one of each being shown in the figure. The F-pilus apparatus, involved in the initial phage reception step, and the peptidoglycan layer are omitted for clarity. OM, outer membrane; IM, inner membrane. B. Schematic representation of the three domains alongside the residue numbering for the mature protein. SS, signal sequence; TMH, transmembrane helix.

FIGURE 2. **Interaction studies of the phage minor coat proteins pIII and pVI.** Bacterial two-hybrid assays were performed in the BTH101 (A) or Oxi-Blue (B) reporter strains producing the indicated proteins or domains (pIII-C, residues 256 to 406; N1, residues 1 to 71; N2, residues 82 to 222; $C_{\Delta TMH}$, residues 256 to 378 of the pIII protein; TolR2-3, residues 45 to 143 of TolR) fused to the T18 or T25 domain of the *Bordetella* adenylate cyclase. Cells were spotted on plates supplemented with IPTG and X-Gal. Interaction between the two fusion proteins is attested by the blue colour. The PgsA-PgsA (A) and TolB-Pal (B) interactions serve as positive controls.

FIGURE 3. **Interactions between pIII, TolQ and TolR.** A. Bacterial two-hybrid assay. BTH101 reporter cells producing the indicated proteins fused to the T18 or T25 domain of the *Bordetella* adenylate cyclase were spotted on plates supplemented with IPTG and X-Gal. Interaction between the

indicated fusion proteins is attested by the blue colour signal. The PgsA-PgsA interaction serves as positive controls. B. Co-purification assay. Triton-solubilised extracts of *E. coli* W3110 WT cells producing pIII fused to the adenylate cyclase T18 domain and HA-tagged TolQ were subjected to immobilisation on calmoduline beads. Left panel: immunodetection of pIII-T18 purification using anti-pIII antibodies. Right panel: immunodetection of TolQ copurification using anti-HA antibodies. C and D. Co-immunoprecipitation assays. Triton-solubilised extracts of *E. coli* W3110 WT cells producing the indicated proteins were subjected to immunoprecipitation with anti-HA (C) or anti-pIII (D) coupled-beads. For B, C and D, the input (total soluble material, TOT) and the immunoprecipitated material (P) were loaded on a 13.5%-acrylamide SDS-PAGE and immunodetected with anti-HA, anti-TolR or anti-pIII antibodies. The molecular weight markers are indicated on the left. A white triangle indicates the signal from the endogenous *tolR* locus. The star mark (*) indicate a protein retained by the beads and non-specifically detected by the polyclonal anti-TolR antibodies.

FIGURE 4. **$TolQ_{HA}$ protease accessibility assay.** $TolQ_{HA}$ was produced in WT *E. coli* cells with or without pIII. Spheroplasts were treated with proteinase K for the indicated time (0, 1, 5 and 10 min). A control sample was incubated with triton and proteinase K for 10 minutes to solubilise the membrane proteins (T). $TolQ_{HA}$ was analysed by SDS-PAGE and immunoblot was performed with anti-HA antibodies. The full-length $TolQ_{HA}$ protein is indicated, as well as the main degradation product $TolQ_{HA}$*. The molecular mass markers (in kDa) are indicated on the left.

FIGURE 5. **Protein-protein interactions between Tol and pIII-C variant proteins.** A. Representation of the pIII-C protein sequence and the various truncated constructs tested. Residues are numerated according to the mature protein. Left panel: schematic representation with secondary structures indicated as arrows (β-strands) or cylinders (α-helices) and named as previously published (21). The endogenous disulfide bond is schematised by a yellow line. ICS: Infection Competence Segment. SS: the 18-residue signal sequence ensures protein insertion in the IM with periplasmic addressing of the N-terminus. Right panel: mapping of the positions of interest on an Alphafold predicted structure of the pIII-C monomer. The disulfide bond stabilising the hairpin in pIII-C is coloured in yellow. Using ChimeraX, the pLDDT colour scheme is represented from blue (bad) to red (good). B. Bacterial two-hybrid assay in BTH101 reporter cells producing the indicated proteins or domains (pIII-C: residues 256 to 406 ; pIII-275: residues 275 to 406 ; pIII-286: residues 286 to 406 ; pIII-308: residues 308 to 406 of pIII) fused to the T18 or T25 domain of the *Bordetella* adenylate cyclase were spotted on plates supplemented with IPTG X-Gal. Interaction between the two fusion proteins is attested by the blue colour. The PgsA-PgsA interaction serves as the positive control.

FIGURE 6. **pIII-C anchor interacts with TolQ TMH2 and TMH3 in a pmf-dependent fashion.** A. Schematic representation of the TMHs of TolQ and pIII-C, highlighting the residues analysed in the

cysteine scanning assay. B. Cells producing the indicated pIII-C cysteine substitution in combination with the $TolQ_{HA}$ cysteine mutations were treated or not with the oxidative agent copper (II) orthophenanthroline (CuOP) to increase dimer formation, then boiled in Laemmli buffer in absence of a reducing agent, loaded onto 12.5% acrylamide SDS-PAGE and immunodetected with anti-HA antibody. The positions of TolQ and TolQ dimer are indicated on the right. The signal susceptible to correspond to the pIII-C/TolQ heterodimer is indicated by a star. C. The pIII-C 382C / $TolQ_{HA}$ 171C sample was re-analysed by cutting the nitrocellulose membrane in two and the signal was immunodetected by either the anti-HA antibodies (right part of the panel) or the anti-pIII antibody (left part of the panel). The molecular weight markers are indicated on the left. D. The experiments were conducted with (+) or without (-) addition of the protonophore CCCP before the CuOP treatment. The molecular weight markers (kDa) are indicated on the left.

FIGURE 7. **pIII-C homodimerization and heterodimerization with TolR.** A. Schematic representation of the TMHs of TolR and pIII-C, highlighting the residues analysed in the cysteine scanning assay. B. Cells producing the indicated pIII-C cysteine substitution in combination with the TolR cysteine mutations were treated with CuOP, then boiled in Laemmli buffer in absence of reducing agent, loaded onto 12.5% acrylamide SDS-PAGE and immunodetected by the anti-TolR polyclonal antibody. The positions of TolR and TolR dimer are indicated on the right. The signal susceptible to correspond to the pIII-C/TolR heterodimer is indicated by a triangle (black: strong signal; white: faint signal). The experiments were conducted with (+) or without (-) addition of the protonophore CCCP before the CuOP treatment. The molecular weight markers (kDa) are indicated on the left.

FIGURE 8. **Mapping of the interaction interfaces between pIIIC, TolQ and tolR**. A. Summary of the interactions observed by cysteine scanning. The TolR anchor (R1), the TolQ transmembrane helices (Q1, Q2 and Q3) and the C-terminal hydrophobic helix of pIII are represented as circles viewed from the periplasm. Residues numbered on the outside of the circles and located at the periplasmic side of the TMHs and were mutated to cysteines. Solid lines indicate strong and reproducible cysteine crosslinking between indicated positions, dashed lines indicate faint interaction signals and red lines are heterocomplexes lost upon treatment with the protonophore CCCP. B. Bacterial two-hybrid assay in the BTH101 reporter cells producing the indicated proteins. The experiment was conducted as described in Figure 2.

Pellegri et al.
Figure 1

A.

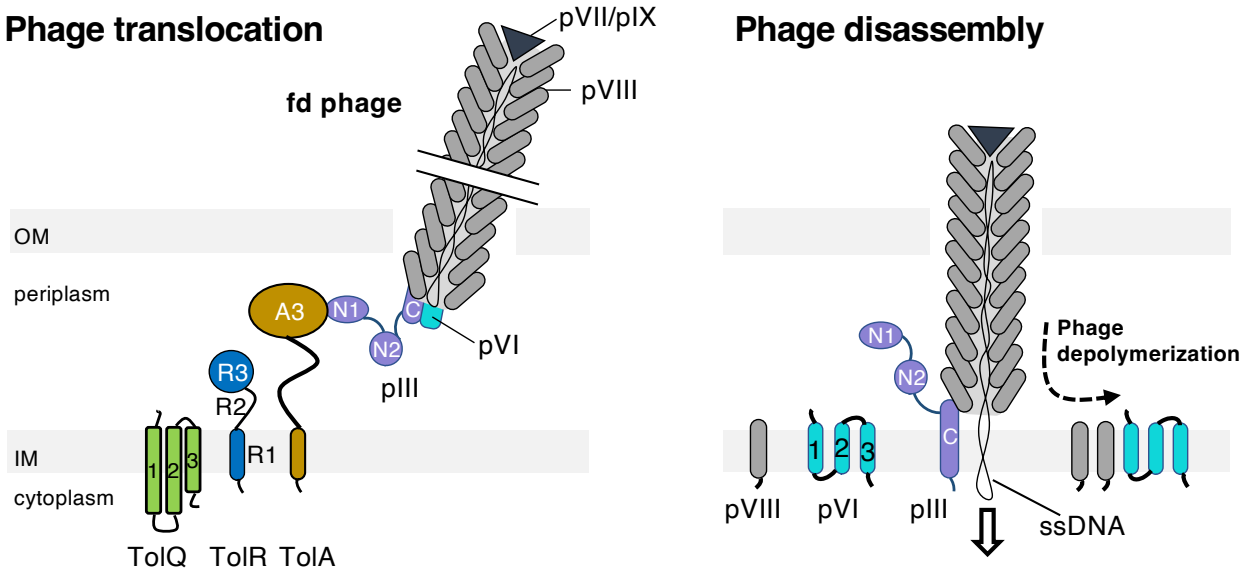

B.

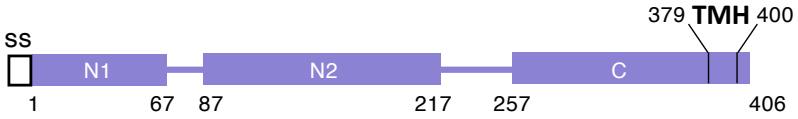

Pellegri et al.
Figure 2

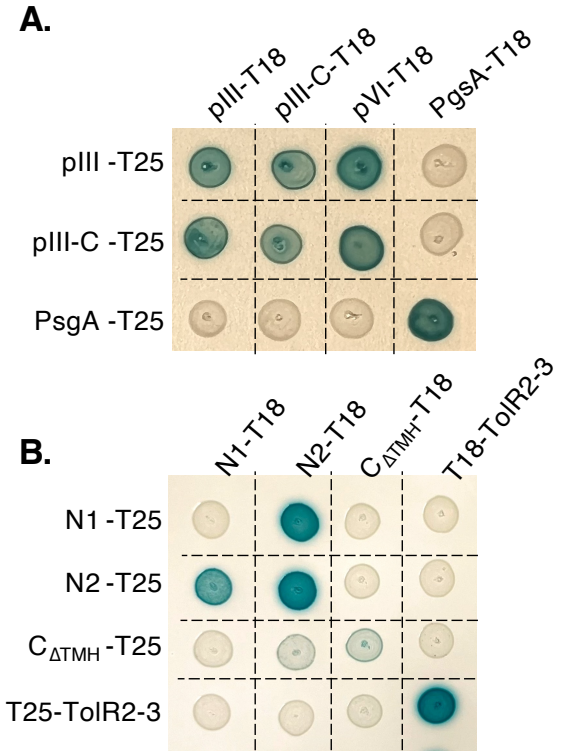

Pellegri et al.
Figure 3

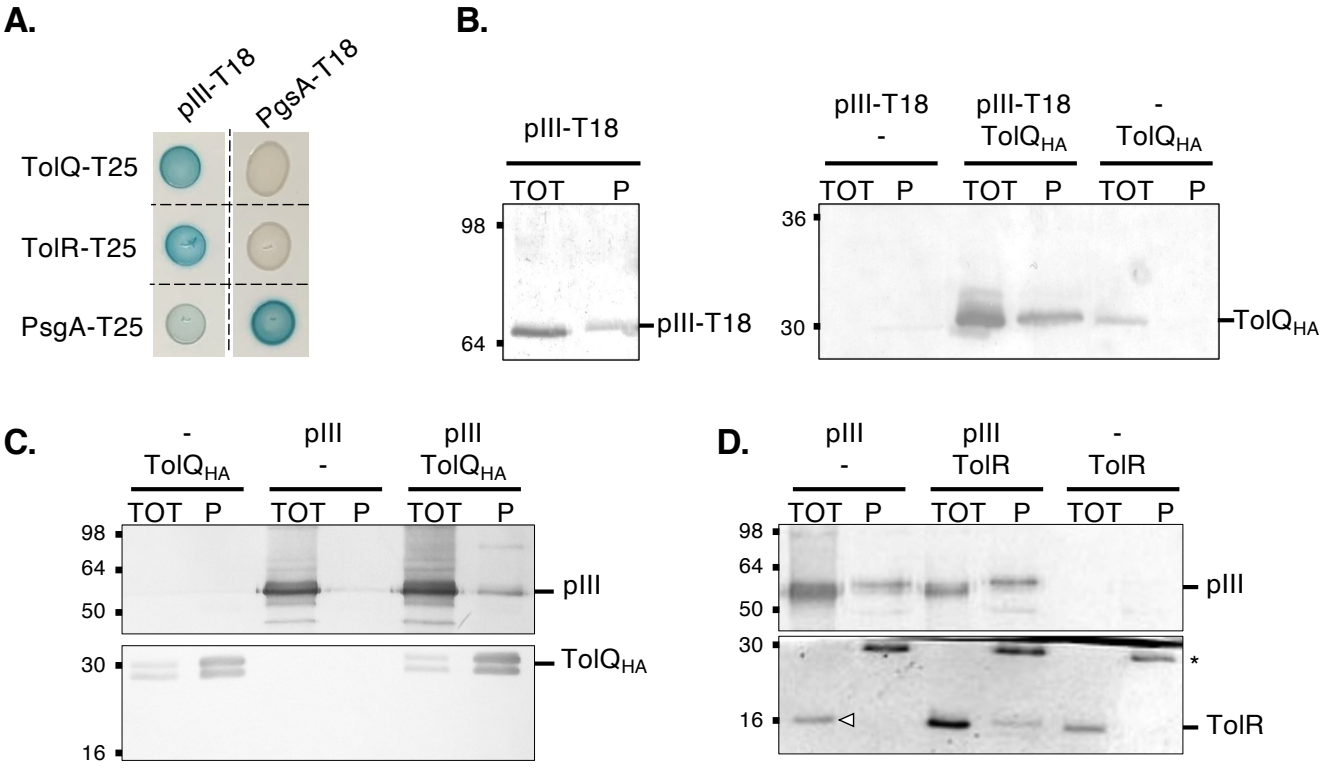

Pellegri et al.
Figure 4

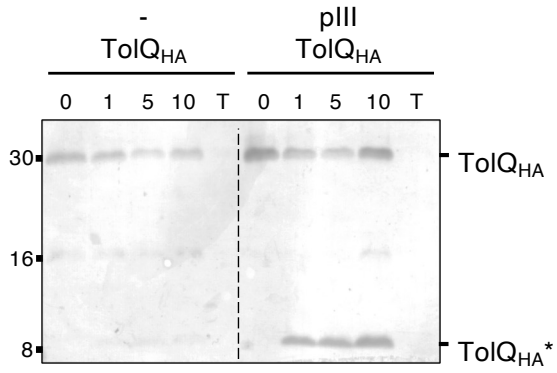

Pellegri et al.
Figure 5

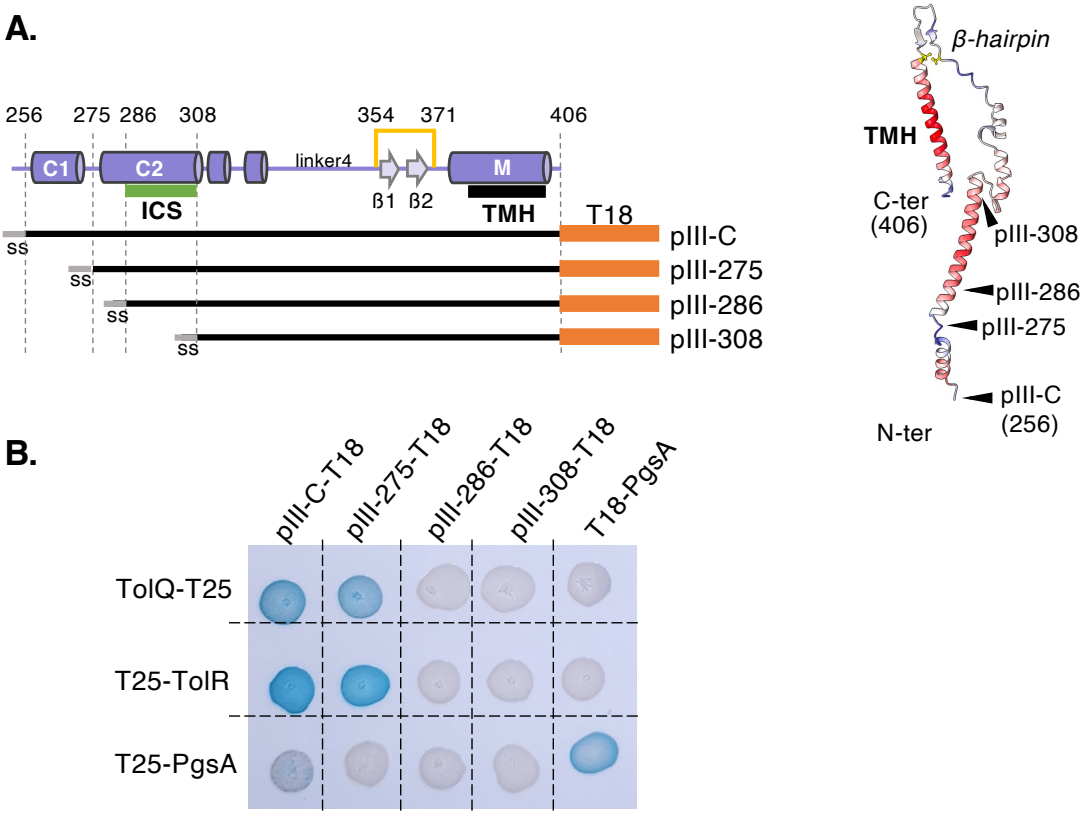

Pellegri et al.
Figure 6

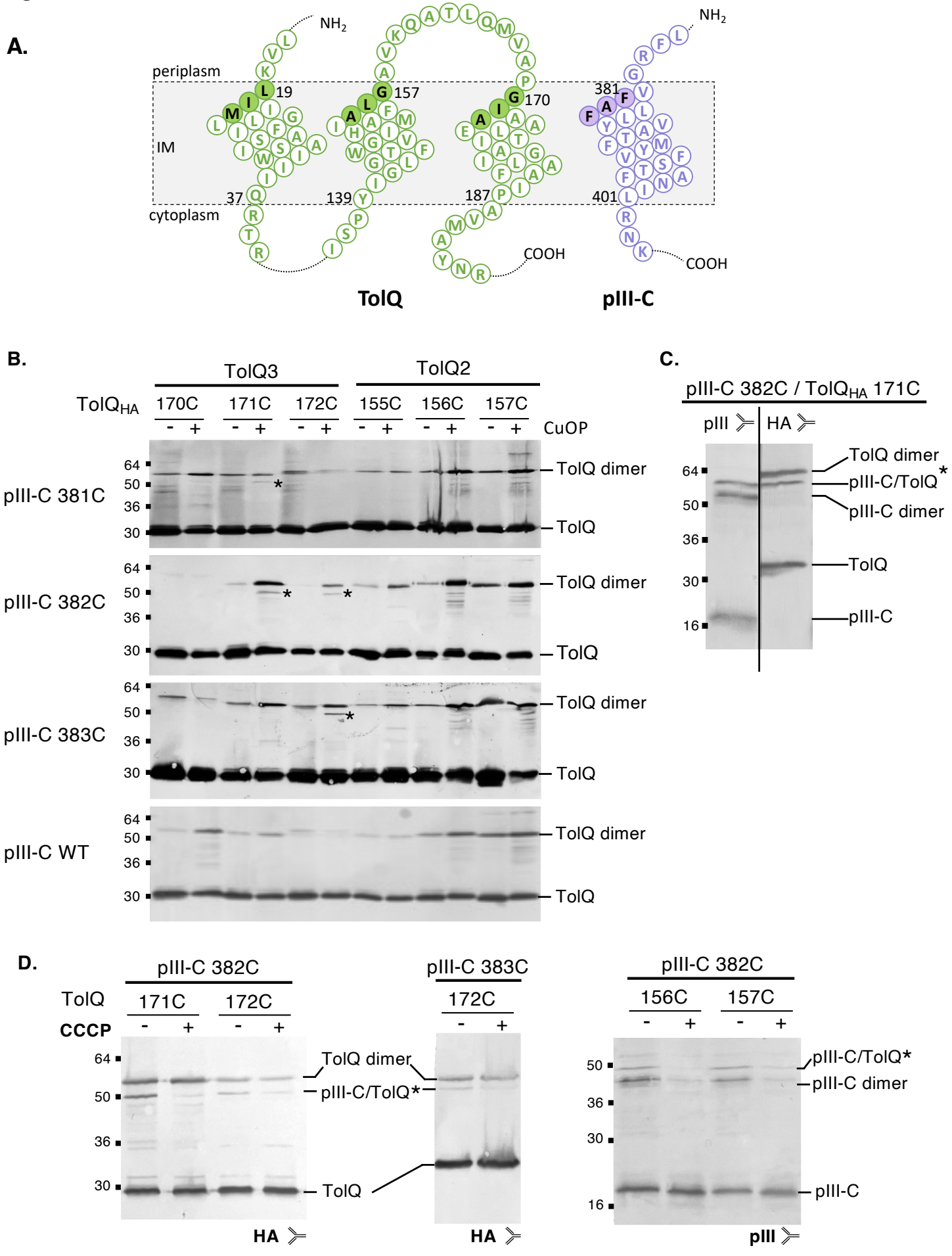

Pellegri et al.
Figure 7

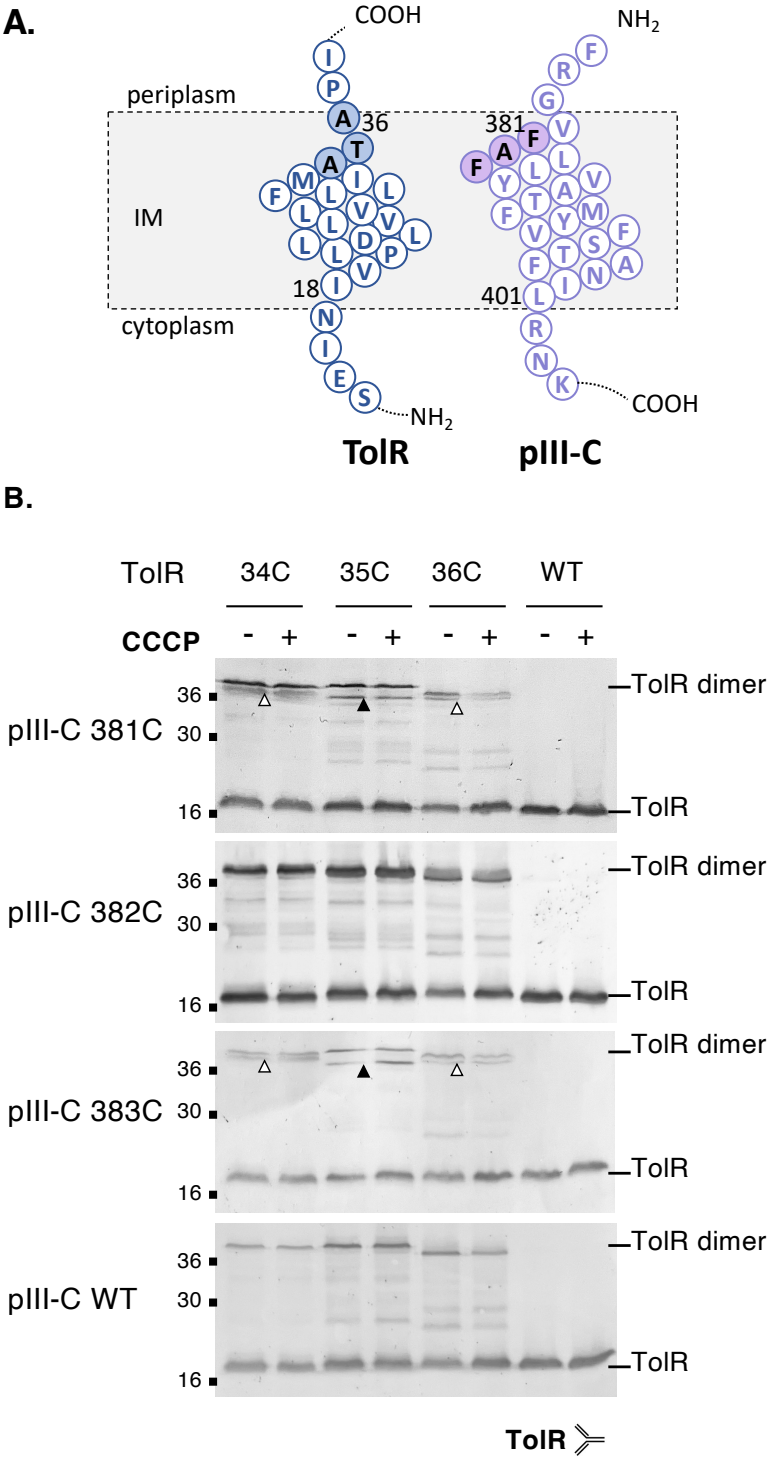

Pellegri et al.
Figure 8

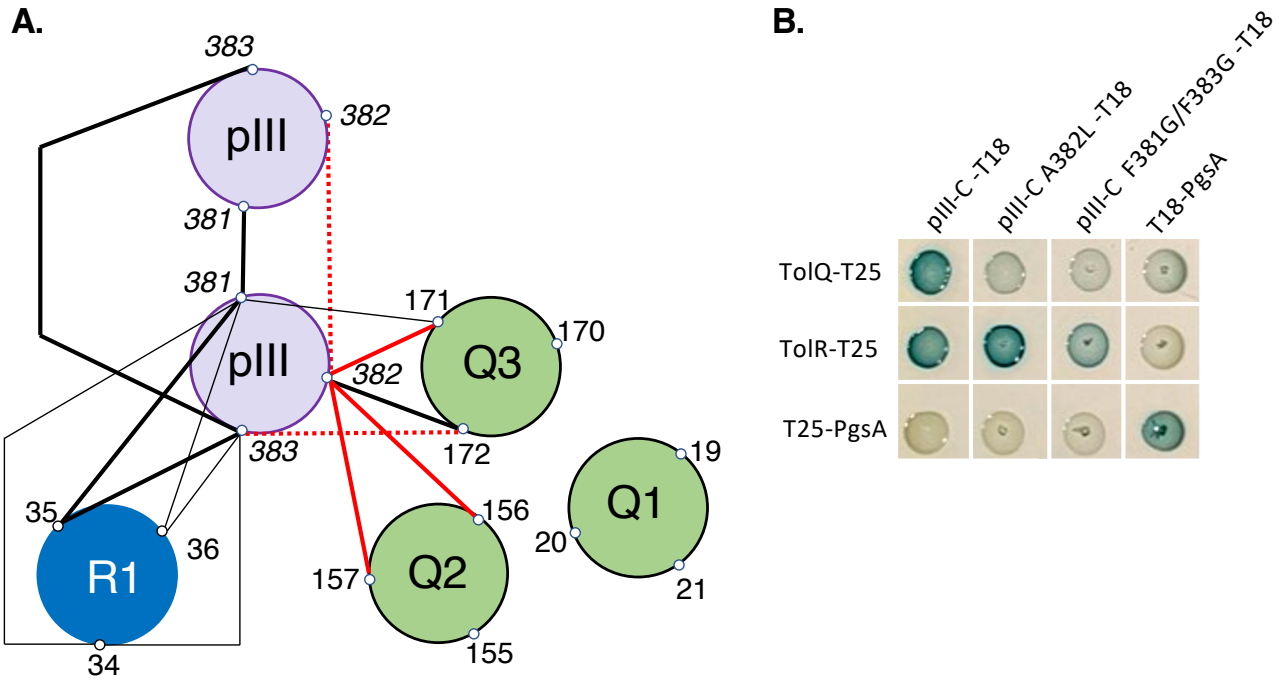

Direct interaction between fd phage pilot protein pIII and the TolQ-TolR proton-dependent motor provides new insights into the import of filamentous phages.

Callypso PELLEGRI, Ambre MOREAU, Denis DUCHE and Laetitia HOUOT

Supporting information

Content:

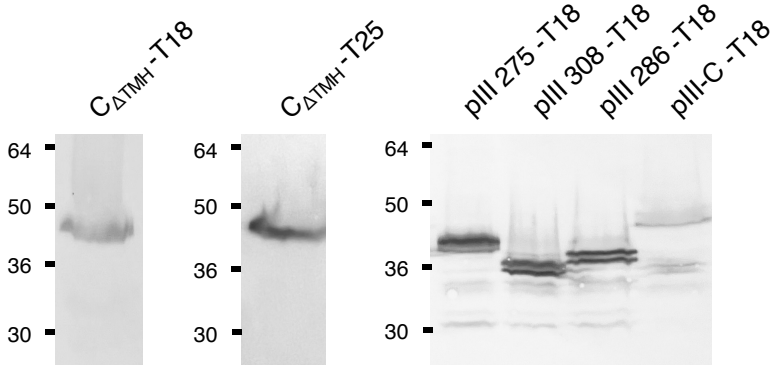

Fig. S1. Protein production level of various BACTH constructs used in this study. Western immunoblot of 0.2 OD units of whole-cell lysates of *E. coli* carrying various inducible expression vectors, and probed with monoclonal anti-Cya 3D1 (T18 constructs) or anti-pIII (NEB, T25 constructs) antibodies. The molecular weight markers (in kDa) are indicated on the left.

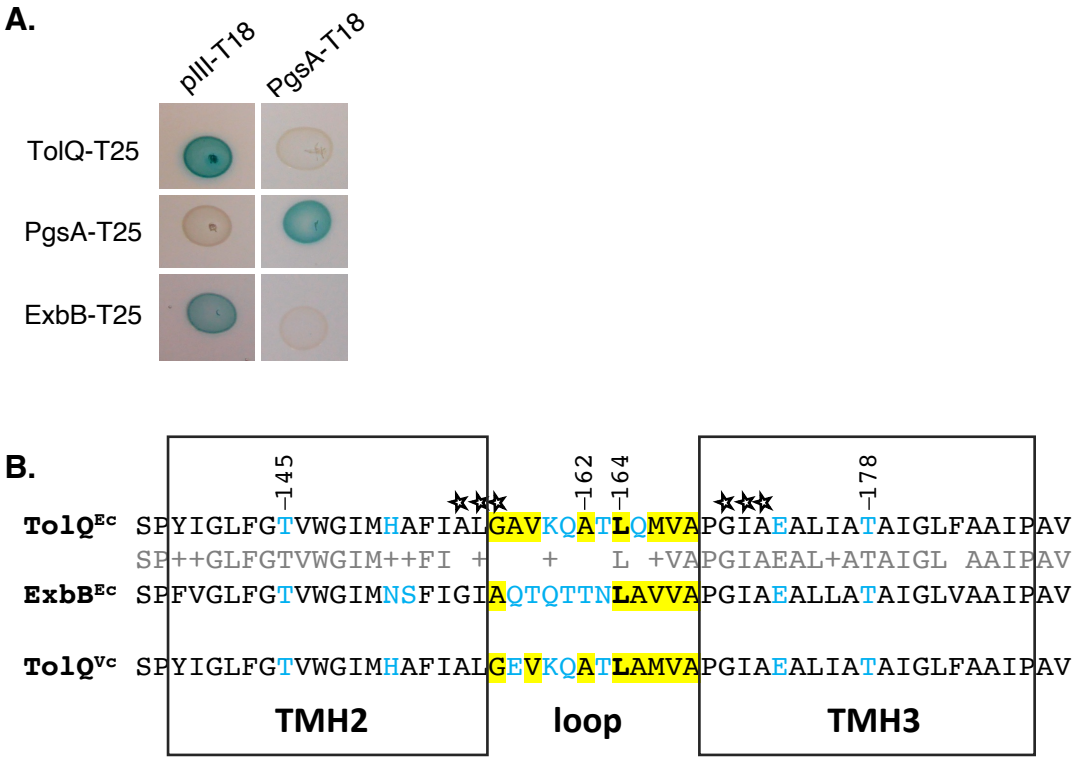

Fig.S2. Cross-talk between TolQ and ExbB for phage uptake. *A*) Bacterial two-hybrid assay in BTH101 reporter cells producing the indicated proteins fused to the T18 or T25 domain of the *Bordetella* adenylate cyclase and spotted on plates supplemented with IPTG X-Gal. PsgA homodimerization serves as a positive control. *B*) Sequence alignment of TolQ and ExbB from *E. coli* or *V. cholerae* and restricted to the periplasmic loop surrounded by the second and third trans-membrane helices (TMH, boxed). Polar residues (blue), hydrophobic residues in the periplasmic loop (yellow), positions mutated in the cysteine-scanning experiment (stars).

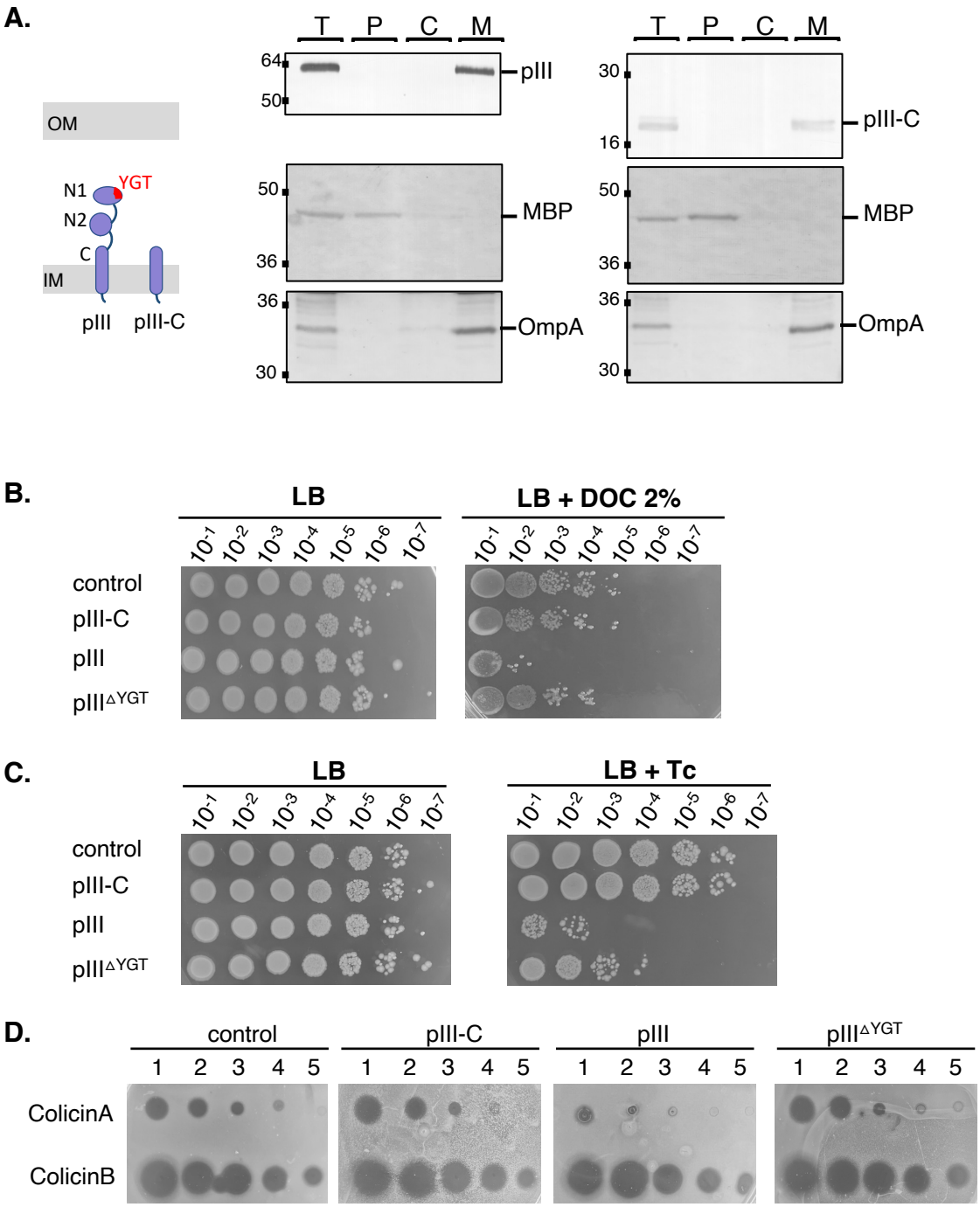

Fig.S3. Phenotypic characterization of GM1 strains producing phage pIII, pIII$^{\Delta YGT}$ or pIII-C proteins. *A*) Fractionation assay attesting the localization of the produced proteins. Left panel is a schematic representation of the protein in the cell envelope. The YGT motif previously identified as essential for pIII-N1/TolA3 interaction is indicated. Central and right panels : the fractions were loaded on a 12.5% acrylamide SDS-PAGE and immunodetected using anti-pIII, anti-MBP and anti-OmpA antibodies. T: total fraction, P: periplasmic, C: cytoplasmic, M: membrane. The molecular weight markers (in kDa) are indicated on the left. B) Cell growth on LB and LB supplemented with deoxycholate 2%. C) Susceptibility to phage infection. Cells were incubated with the phage during 30 min, 10-fold serial diluted and spotted on LB plates and on LB plates supplemented with tetracycline (LB+Tc, right panel), in order to numerate the total number of CFU, and fd-Tc phage infected CFU, respectively. Experiments were conducted in triplicate. D) Colicin sensitivity was estimated by 5-fold serial spot dilutions. One microliter of colicin (A or B) was spotted on to a growing lawn of cells. Clear zones indicate cell death. ColA is dependent on the Tol system while ColB is dependent on the TonB-ExbBD system for uptake.

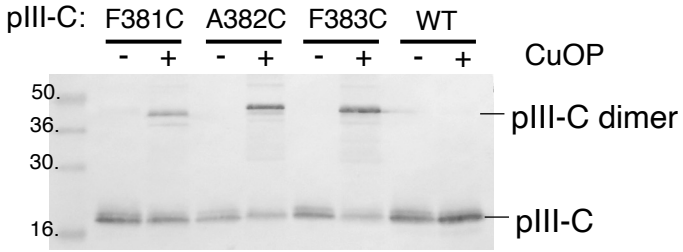

Fig. S4: Dimerization of pIII-C visualized by in vivo disulfide bond formation .
Cells producing the indicated pIII-C cysteine substitution were treated or not with the oxidative agent copper (II) orthophenanthroline to increase dimer formation, then boiled in Laemmli buffer in absence of reducing agent, loaded onto 12.5% acrylamide SDS-PAGE and immunodetected with anti-pIII antibody. The molecular weight markers (in kDa) are indicated on the left.

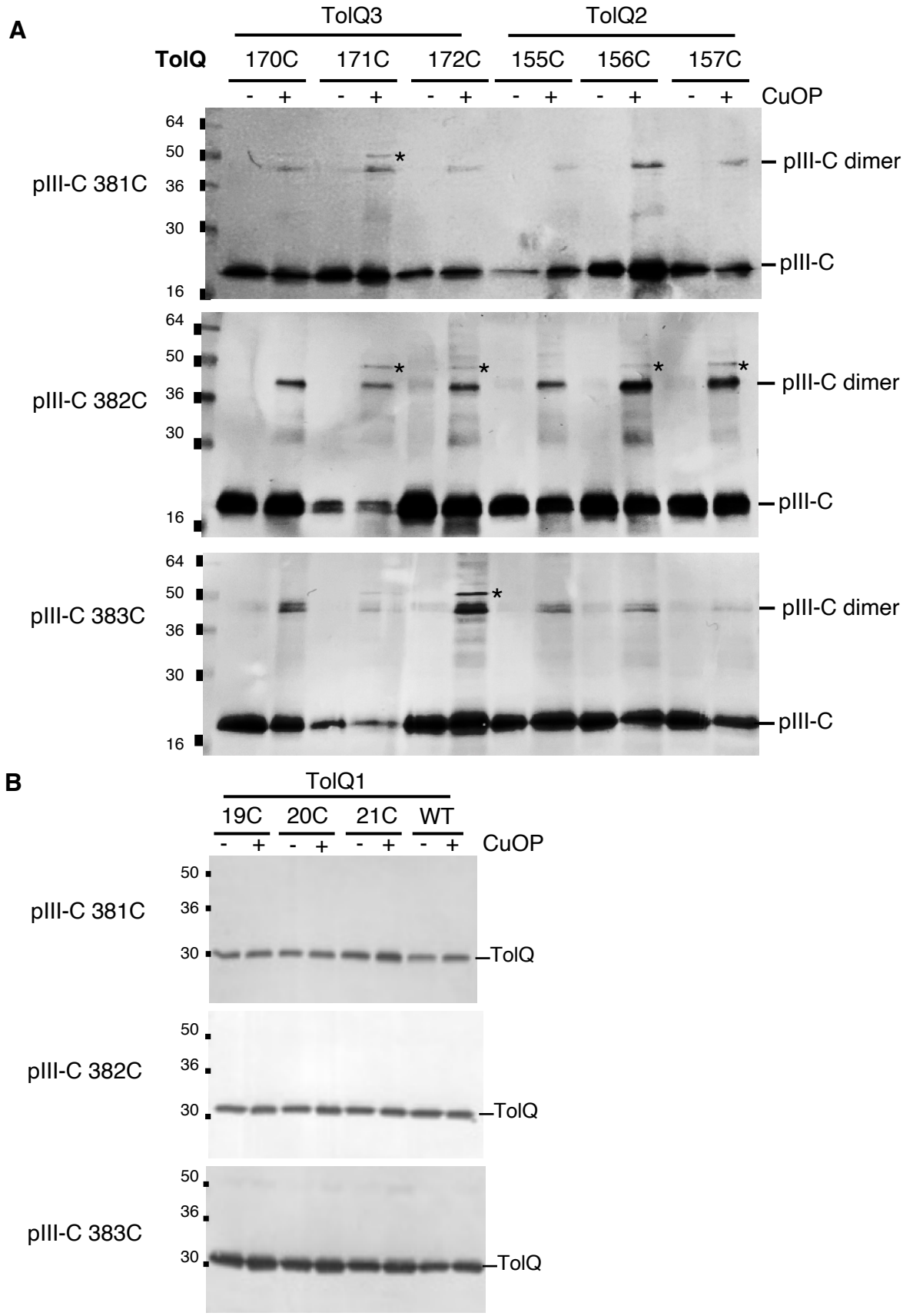

Fig. S5: pIII-C interacts with TolQ TMH2 and TMH3 but not TMH1.

Cells producing the indicated pIII-C cysteine substitution in combination with the $TolQ_{HA}$ cysteine mutations in TolQ2 and TolQ3 (A) or TolQ1 (B) were treated or not with the oxidative agent copper (II) orthophenanthroline (CuOP) to increase dimer formation, then boiled in Laemmli buffer in absence of reducing agent, loaded onto 12.5% acrylamide SDS-PAGE and immunodetected with the anti-pIII (A) or anti HA antibody (B). The positions of pIII-C and pIII-C dimer are indicated on the right. The signal susceptible to correspond to the pIII-C/TolQ heterodimer is indicated by a star. The molecular weight markers (in kDa) are indicated on the left.

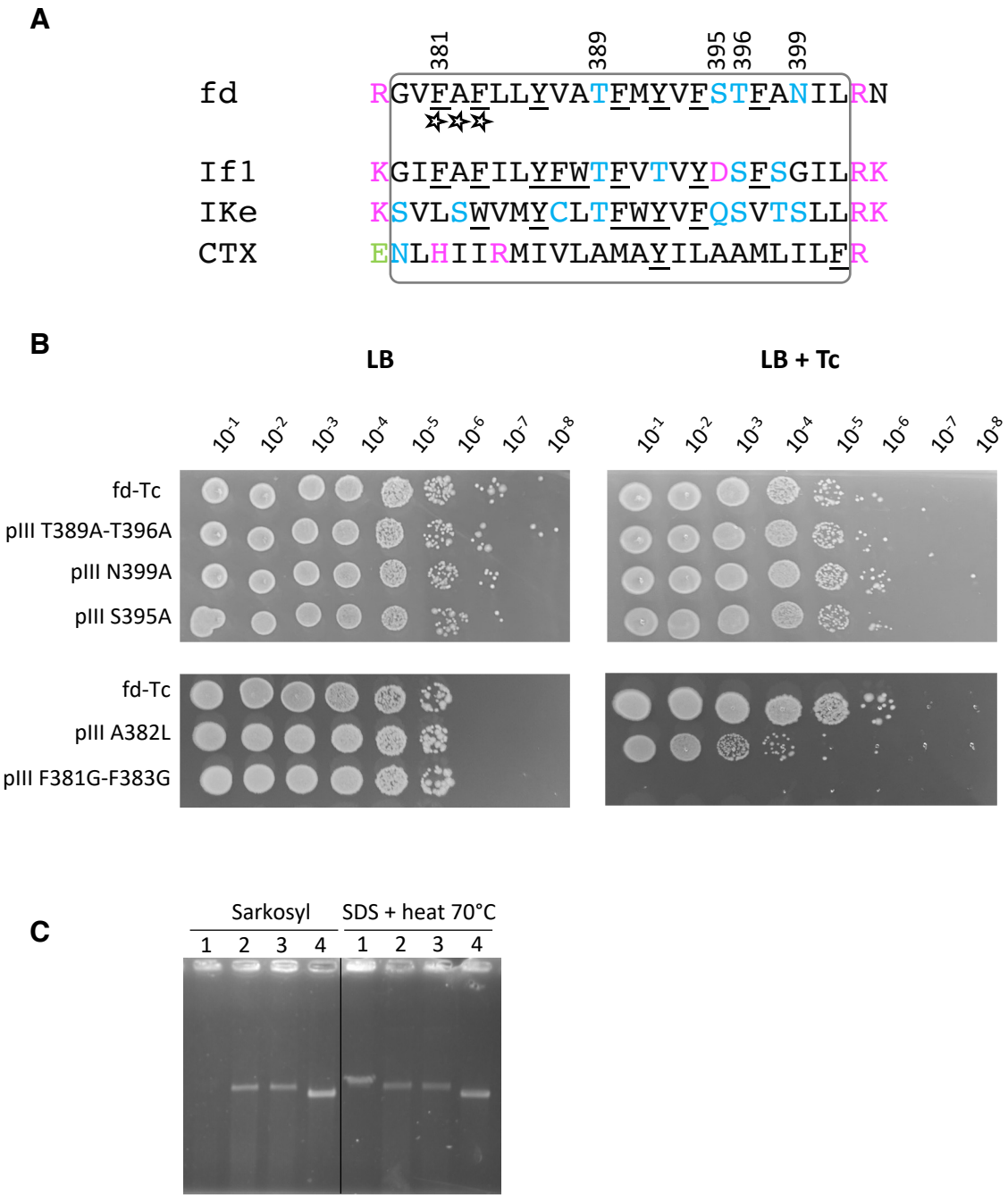

Fig. S6: Analysis of pIII C-terminal membrane anchor. A. Sequence alignment of filamentous phage predicted TMHs. The hydrophobic helix of the coliphages fd, If1, Ike and the vibriophage CTX are presented boxed. Polar residues (blue), aromatic residues (underlined), acidic residues (green), basic residues (pink), positions mutated in the cysteine-scanning experiments (Fig. 6 and 7) and in the phage infection assay (stars).
B. Host susceptibility to phage mutants. GM1 F^+ cells were incubated with the WT fd-Tc phages or the indicated virion mutants during 30 min, 10-fold serial diluted and spotted on LB plates and on LB plates supplemented with tetracycline (LB+Tc, right panel), in order to numerate the total number of CFU, and of fd-Tc phage infected CFU, respectively. Experiments were conducted in triplicate.
C. Phage virions stability assay by native agarose gel electrophoresis. Virions particles were produced with wild-type pIII (1), pIII A382L (2), pIII F381G-F383G (3) or pIII-286 (4). Virions were incubated either with sarkosyl 0.1% for 10 min (left panel) or with SDS 1% and heated at 70°C for 15 min (right panel) prior to electrophoresis on a 0.6% agarose gel. Released ssDNA from destabilized virions can be visualized by gelred staining. The phage sample pIII-286 used as a control was previously shown to be unstable and to release its genome in the presence of sarkosyl detergent (Rakonjac et al. 1999).

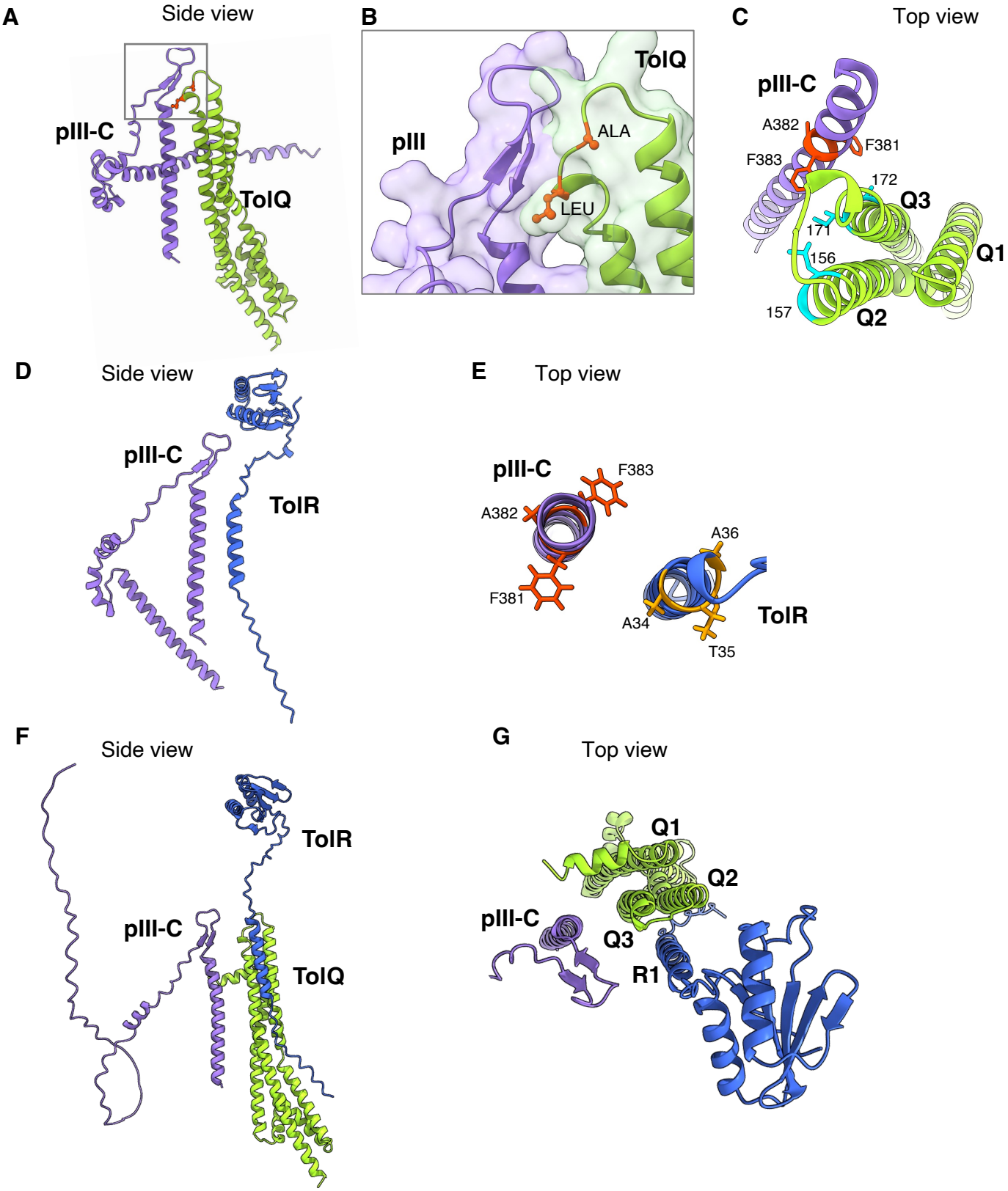

Fig. S7: Modelization of pIII interaction with TolQ and TolR.
Alphafold predictions of the pIII-C domain (coloured in purple), TolQ (yellow-green) and TolR (blue). In the predicted pIII-C/TolQ complex, pIII-C terminal TMH is positioned obliquely to TolQ TMH2 and TMH3, with the β-hairpin hiding part of the TolQ periplasmic loop. The boxed region is detailed in panel B, with the TolQ residues Ala162 and Leu164 colored in red. The pIII-C/TolR complex prediction is presented in panel D. Panel C and E are top views of the complexes from the periplasm. Residues mutated in the cysteine crosslinking experiment are indicated (C and E). The prediction comprising pIII-C, TolQ and TolR (panel F and G) identify the TolQ/TolR heterocomplex, but excludes pIII-C from the structure.

		Total CFU	SD	Infected CFU/mL	SD	F	SD
W3110	CCCP -	1.33 x 10E+10	6.11 x 10E+09	7.85 x 10E+03	2.17 x 10E+03	6.21 x 10E-07	1.08 x 10E-07
W3111	CCCP +	1.60 x 10E+10	6.93 x 10E+09	4.7 x 10E+01	2.31 x 10E+01	2.83 x 10E-09	2.89 x 10E-10

Table S1. Effect of the CCCP on the infection frequency for the W3110 F^- strain . Cells pretreated or not with the protonophore CCCP 10 μM were incubated with the fd-Tc phage in the presence of $CaCl_2$ during 15 min, 10-fold serial diluted and spotted on LB plates to numerate total CFU, and LB plates supplemented with tetracycline to numerate the fd-Tc infected CFU, respectively. Experiments were conducted in triplicate. The frequency of infection (F) was calculated as the mean of the 3 infection with standard deviation (SD).

Table S2: Strains, plasmids and oligonucleotides

Strain, plasmid or library	Genotype or description	Reference or source
***E. coli* strains and phages**		
DH5α	F$^-$ Φ80*lac*ZΔM15 Δ(*lac*ZYA-*arg*F) U169 *rec*A1 *end*A1 *hsd*R17 (rK–, mK+) *pho*A *sup*E44 λ– *thi*-1 *gyr*A96 *rel*A1	Laboratory collection
W3110	F- lambda- IN(rrnD-rrnE)1 rph-1	Laboratory collection
W3110 Δ*tolQRΔexbBD*	W3110 strain deleted of *tolQ*, *tolR* and *exbB, exbD* genes	Samire *et al.,* 2020
GM1	*ara, thi,Δ(lac pro), F', lac, pro*	Laboratory collection
BTH101	F-, cya-99, araD139, galE15, galK16, rpsL1 (StrR), hsdR2, mcrA1, mcrB1.	Laboratory collection
Oxi-Blue	Shuffle T7 Express (*fhuA2 lacZ::T7 gene1* [lon] *ompT ahpC gal λatt*::pNEB3-r1-*cDsbC* (Spec^R, lacI^q) *ΔtrxB* sulA11 *R(mcr-73::miniTn10*--Tet^S)2 [dcm] *R(zgb-210::Tn10* --Tet^S) *endA1 Δgor Δ(mcrC-mrr)114::IS10), Δcya, ΔphoA lacZ*$^+$	Pellegri *et al.,* unpublished
fd-Tc	fd phage carrying a tetracyclin resistance gene	ATCC 37000
fd-Tc pIII T389A T396A	fd-Tc bearing a T-to-A substitution at position 389 and 395 in pIII	This study
fd-Tc pIII N399A	fd-Tc bearing a N-to-A substitution at position 369 in pIII	This study
fd-Tc pIII S395A	fd-Tc bearing a S-to-A substitution at position 399 in pIII	This study
fd-Tc pIIIΔN2	fd-Tc deleted of the pIII-N2 domain (residues 72 to 256).	This study
fd-Tc pIII A382L	fd-Tc bearing a A-to-L substitution at position 382 in pIII	This study
fd-Tc pIII F381G/F383G	fd-Tc bearing a F-to-G substitution at position 381 and 383 in pIII	This study
fd-Tc pIII-286	fd-Tc bearing a deletion of residues 1 to 285 in pIII. The virion is unstable in the presence of sarkosyl 0.1%.	This study, based on Rakonjac *et al*. 1999
Plasmids used		
pOK12	IPTG-inducible plasmid, KanR	Vieira and Messing, 1991
pBAD/HisC	pBR322-derived expression vector, L-arabinose inducible, AmpR	Invitrogen
pKT25	BACTH expression vector encoding T25 fragment of *B. pertussis cyaA*; Km^R	Karimova *et al*., 1998
pUT18	BACTH expression vector encoding T18 fragment of *B. pertussis cyaA*; Amp^R	Karimova *et al*., 1998
pUT18C	Modified version of pUT18 with the polylinker located on the C-terminal end of T18	Karimova *et al*., 1998
Two-hybrid constructions		
pIII-T18	fd pIII sequence cloned upstream T18 into pUT18	This study
pIIIC-T18	fd pIII sequence (residues 256 to 406) cloned upstream T18 into pUT18	This study
pVI-T18	fd pIII sequence cloned upstream T18 into pUT18C	This study
N1-T18	fd pIII sequence (residues 1 to 71) cloned upstream T18 into pUT18C	This study
N2-T18	fd pIII sequence (residues 82 to 222) cloned upstream T18 into pUT18	This study
C_{ATM}-T18	fd pIII sequence (residues 256 to 378) cloned upstream T18 into pUT18	This study
pIII275-T18	fd pIII sequence (residues 275 to 406) cloned upstream T18 into pUT18	This study
pIII286-T18	fd pIII sequence (residues 286 to 406) cloned upstream T18 into pUT18	This study
pIII308-T18	fd pIII sequence (residues 308 to 406) cloned upstream T18 into pUT18	This study
pIIIC-T18 A382L	pIIIC-T18 plasmid bearing a A-to-L substitution at position 382 in pIII	This study
pIIIC-T18 F383W	pIIIC-T18 plasmid bearing a F-to-W substitution at position 383 in pIII	This study
pIIIC-T18 F381G F383G	pIIIC-T18 plasmid bearing a F-to-G substitution at position 381 and 383 in pIII	This study
T18-TolR2-3	*E.coli* TolR sequence (residues 45 to 143) cloned downstream T18 into pUT18	Battesti and Bouveret. 2008
PgsA-T18	*E.coli* PgsA sequence cloned upstream T18 into pUT18	Battesti and Bouveret. 2008
pIII-T25	fd pIII sequence cloned upstream T25 into pKT25	This study
pIIIC-T25	fd pIII sequence (residues 256 to 406) cloned upstream T25 into pKT25	This study
N1-T25	fd pIII sequence (residues 1 to 71) cloned upstream T25 into pKT25	Houot *et al.,* 2017
N2-T25	fd pIII sequence (residues 82 to 222) cloned upstream T25 into pKT25	This study
C_{ATM}-T25	fd pIII sequence (residues 256 to 378) cloned upstream T25 into pKT25	This study
TolQ-T25	*E.coli* TolQ sequence cloned upstream T25 into pKT25	This study
T25-TolR	*E.coli* TolR sequence cloned downstream T25 into pKT25	This study
T25-TolR2-3	*E.coli* TolR sequence (residues 45 to 143) cloned downstream T25 into pKT25	Battesti and Bouveret. 2008
ExbB-T25	*E.coli* ExbB sequence cloned upstream T25 into pKT25	This study
PgsA-T25	*E.coli* PgsA sequence cloned upstream T25 into pKT25	Battesti and Bouveret. 2008
Co-IP, physiology and infection assay constructions		
pOK-TolQ^{HA}	pOK12 plasmid carrying the *E. coli tolQ* gene fused to an HA tag, Kan^R	Zhang *et al*., 2011
pOK-TolR	pOK12 plasmid carrying the *E. coli tolR* gene, Kan^R	Zhang *et al*., 2009
pBAD-pIII	pBAD/HisC plasmid carrying the fd *pIII* gene, Amp^R	This study
pBAD-pIIIC	pBAD/HisC plasmid carrying the fd *pIII* gene fragment coding residues 275 to 406, Amp^R	This study
pBAD-pIII$^{\Delta YGT}$	Deletion of the sequence encoding the pIII YGT motif (residues 54 to 56) in the pBAD-pIII plasmid, AmpR	This study
Cystein scanning constructions		
pBAD-pIIIC-F381C	pBAD-pIIIC plasmid bearing a F-to-C substitution at position 381 in pIIIC, Amp^R	This study
pBAD-pIIIC-A382C	pBAD-pIIIC plasmid bearing a A-to-C substitution at position 382 in pIIIC, Amp^R	This study
pBAD-pIIIC-F383C	pBAD-pIIIC plasmid bearing a F-to-C substitution at position 383 in pIIIC, Amp^R	This study
pOK-TolQ^{HA}-L19C	pOK-TolQ^{HA} plasmid bearing a L-to-C substitution at position 19 in TolQ, Kan^R	Zhang *et al*., 2011

pOK-TolQ^{HA}-I20C	pOK-TolQ^{HA} plasmid bearing a I-to-C substitution at position 20 in TolQ, Kan^{R}	Zhang *et al*., 2011
pOK-TolQ^{HA}-M21C	pOK-TolQ^{HA} plasmid bearing a M-to-C substitution at position 21 in TolQ, Kan^{R}	Zhang *et al*., 2011
pOK-TolQ^{HA}-A155C	pOK-TolQ^{HA} plasmid bearing a A-to-C substitution at position 155 in TolQ, Kan^{R}	Zhang *et al*., 2011
pOK-TolQ^{HA}-L156C	pOK-TolQ^{HA} plasmid bearing a L-to-C substitution at position 156 in TolQ, Kan^{R}	Zhang *et al*., 2011
pOK-TolQ^{HA}-G157C	pOK-TolQ^{HA} plasmid bearing a G-to-C substitution at position 157 in TolQ, Kan^{R}	Zhang *et al*., 2011
pOK-TolQ^{HA}-G170C	pOK-TolQ^{HA} plasmid bearing a G-to-C substitution at position 170 in TolQ, Kan^{R}	Zhang *et al*., 2011
pOK-TolQ^{HA}-I171C	pOK-TolQ^{HA} plasmid bearing a I-to-C substitution at position 171 in TolQ, Kan^{R}	Zhang *et al*., 2011
pOK-TolQ^{HA}-A172C	pOK-TolQ^{HA} plasmid bearing a A-to-C substitution at position 172 in TolQ, Kan^{R}	Zhang *et al*., 2011
pOK-TolR-A34C	pOK-TolR plasmid bearing a A-to-C substitution at position 34 in TolR, Kan^{R}	Zhang *et al*., 2009
pOK-TolR-T35C	pOK-TolR plasmid bearing a T-to-C substitution at position 35 in TolR, Kan^{R}	Zhang *et al*., 2009
pOK-TolR-A36C	pOK-TolR plasmid bearing a A-to-C substitution at position 36 in TolR, Kan^{R}	Zhang *et al*., 2009

Oligonucleotide	**Name**	**Sequence (5' → 3')**
pIII-T18	oLH456	gcggataacaatttcacacaggaaacagctATGAAAAAATTATTATTCGCAATTCC
	oLH457	GGCGGCTGAATTCGAGCTCGGTACCgcAGACTCCTTATTACGCAGTATGTTAGC
pIIIC-T18	oLH489	AGTTGTTCCTTTCTATTCTCACTCCGCTTCCGGTGATTTTGATTATGAAAAAATGGC
	oLH490	GCCATTTTTTCATAATCAAAATCACCGGAAGCGGAGTGAGAATAGAAAGGAACAACT
pVI-T18	oLH468	caatttcacacaggaaacagctATGACCATGCCAGTTCTTTTGGGTATTCCG
	oLH469	GCTCGGTACCCGGGGATCCTCTAGAGTTTTATCCCAATCCAAATAAGAAACG
N1s-T18	oLH517	GAACGCCACTGCAGGTCGACTCTAGCTGAAACTGTTGAAAGTTGTTTAGC
	oLH518	GAATTCGAGCTCGGTACCCGGGGATCCTGAGCCACCACCCTCATTTTCAGG
N2s-T18	oLH519	CTGCAGGTCGACTCTAGAGGATCCCTCTGAGGGTGGCGGTACTAAACCTC
	oLH520	CCCGTGGCCTCGCTGGCGGCTGAATTCGAACCAGAGCCGCCGCCAGCATTGA
Cs-T18	oLH515	cagctATGACCATGATTACGCCAAGCGATTTTGATTATGAAAAAATGGC
	oLH516	CCTCTAGAGTCGACCTGCAGGCATGCAAACGGAATAAGTTTATTTTGTCAC
pIII132-T18	oLH511	CCTTTAGTTGTTCCTTTCTATTCTCACTCCgcaGCCGATGAAAACGCGCTACAGTCTG
	oLH512	GAATAGAAAGGAACAACTAAAGGAATTGCG
pIII121-T18	oLH491	AGTTGTTCCTTTCTATTCTCACTCCGCTGGCAAACTTGATTCTGTCGCTACTGATTACG
	oLH492	CGTAATCAGTAGCGACAGAATCAAGTTTGCCAGCGGAGTGAGAATAGAAAGGAACAACT
pIII93-T18	oLH493	AGTTGTTCCTTTCTATTCTCACTCCGCTGGCCTTGCTAATGGTAATGGTGCTACTGG
	oLH494	CCAGTAGCACCATTACCATTAGCAAGGCCAGCGGAGTGAGAATAGAAAGGAACAACT
pIII-T25	oLH502	CCAGCCTGATGCGATTGCTGCATGGTtgctcctgctccACGGAATAAGTTTATTTTGTCAC
	oLH503	GTTTGCGTAACCAGCCTGATGCGATTGCTGtcctcctcctgctgctgcAGACTCCTTATTACGCAGTATGTTAGC
pIIIC-T25	oLH489	AGTTGTTCCTTTCTATTCTCACTCCGCTTCCGGTGATTTTGATTATGAAAAAATGGC
	oLH490	GCCATTTTTTCATAATCAAAATCACCGGAAGCGGAGTGAGAATAGAAAGGAACAACT
N2s-T25	oLH521	CTGCAGGGTCGACTCTAGAGGATCCCtctgagggtggcggtactaaacctc
	oLH522	aaaacgacggccgaattcttagTTAcgaccagagccgccgccagcattgac
Cs-T25	oLH513	ggataacaatttcacacaggaaacagctATGGATTTTGATTATGAAAAAATGGC
	oLH514	CCAGCCTGATGCGATTGCTGCATGGTtgctcctgctccACGGAATAAGTTTATTTTGTCAC
TolQ-T25	oLH504	caatttcacacaggaaacagctATGGTGACTGACATGAATATCCTTG
	oLH506	CAGCCTGATGCGATTGCTGCATGGTCCCCTTGTTGCTCTCGCTAAC
TolR-T25	oLH204	GTCGACTCTAGAGGATCCCCGGGTACCTAAGGCCAGAGCGCGTGGACGAGGT
	oLH205	gacgttgtaaaacgacggccgaattcttagTTAGATAGGCTGCGTCATTAAAC
ExbB-T25	oLH202	GCGGATAACAATTTCACACAGGAAACAGCTGTGGGTAATAATTTAATGCAGACGG
	oLH203	ACCAGCCTGATGCGATTGCTGCATGGTCATTCCTGCGCGTAATTTTTGTGCGAC
pIIIC-T18 A382L	oLH596	ATAAACTTATTCCGTGGTGTCTTTctGTTTCTTTTATATGTTGCCACC
	oLH598	AAAGACACCACGGAATAAGTTTATTTTGTCAC
pIIIC-T18 F381G F383G	oLH602	GTGACAAAATAAACTTATTCCGTGGTGTCggTGCGggtCTTTTATATGTTGCCACCTTTATGTATG
	oLH603	CCACGGAATAAGTTTATTTTGTCACAATCAATAGAAAATTC
pBAD-pIII	oLH474	GGGCTAACAGGAGGAATTAACCATGGTGAAAAAATTATTATTCGCAATTCC
	oLH475	CTGTCCACCAGTCATGCTAGCCATACCttaAGACTCCTTATTACGCAGTATG
pBAD-pIIIC	oLH489	AGTTGTTCCTTTCTATTCTCACTCCGCTTCCGGTGATTTTGATTATGAAAAAATGGC
	oLH490	GCCATTTTTTCATAATCAAAATCACCGGAAGCGGAGTGAGAATAGAAAGGAACAACT
pBAD-pIIIC-F381C	oLH383	CTTATTCCGTGGTGTCTGTGCGTTTCTTTTATATG
	oLH384	ACGGAATAAGTTTATTTTGTCACAATC
pBAD-pIIIC-A382C	oLH395	CCGTGGTGTCTTTtgcTTTCTTTTATATGTTGCC
	oLH398	AAAGACACCACGGAATAAGTTTATTTTGTCAC
pBAD-pIIIC-F383C	oLH396	CCGTGGTGTCTTTGCGtgtCTTTTATATGTTGCC
	oLH398	AAAGACACCACGGAATAAGTTTATTTTGTCAC
fd-Tc pIII T389A T395A	oLH569	GCAAACGCCGAAAATACATACATAAAGGCGGCAACATATAAAAGAAACGC
	oLH570	GCCGCCTTTATGTATGTATTTTCGGCGTTTGCTAACATACTGCGTAATAAGG
fd-Tc pIII N369A	oLH571	CGACGTTTGCTgcCATACTGCGTAATAAGGAGTC
	oLH572	CGCAGTATGgcAGCAAACGTCGAAAATACATAC
fd-Tc pIII S399A	oLH472	ATTTGCGACGTTTGCTAACATACTGCG
	oLH473	CGTCGCAAATACATACATAAAGGTGG
fd-Tc pIII A382L	oLH596	ATAAACTTATTCCGTGGTGTCTTTctGTTTCTTTTATATGTTGCCACC
	oLH598	AAAGACACCACGGAATAAGTTTATTTTGTCAC
fd-Tc pIII F381G F383G	oLH602	GTGACAAAATAAACTTATTCCGTGGTGTCggTGCGggtCTTTTATATGTTGCCACCTTTATGTATG
	oLH603	CCACGGAATAAGTTTATTTTGTCACAATCAATAGAAAATTC
fd-Tc pIIIΔN2	oLH487	GGCGGTTCTGAGGGTGGCGGTTCTGATGGCGGCTCCGGTTCCGGTGATTTTG
	oLH488	CAAAATCACCGGAACCGGAGCCGCCATCAGAACCGCCACCCTCAGAACCGCC
fd-Tc pIII-286	oLH491	AGTTGTTCCTTTCTATTCTCACTCCGCTGGCAAACTTGATTCTGTCGCTACTGATTACG
	oLH492	CGTAATCAGTAGCGACAGAATCAAGTTTGCCAGCGGAGTGAGAATAGAAAGGAACAACT

Experimental procedures

Cell fractionation. Cell fractionation was performed as previously described (55). The membrane pellet was resuspended in 1 ml of 1 M carbonate sodium (Na_2CO_3) and incubated on a rotating wheel for 30 min at room temperature. Ultracentrifugation at 90,000 g for 40 min then separated the integral membrane fraction (pellet) from the membrane-associated fraction (supernatant). The periplasmic, cytoplasmic, and membrane-associated fractions were precipitated with 15% trichloroacetic acid and resuspended in loading buffer prior to analysis by SDS-PAGE and immunoblotting.

Sensitivity test to DOC. Strains carrying the plasmid of interest were cultivated in the presence of L-arabinose (0.02%) to induce protein expression until they reached OD_{600nm}=0.6. Normalized cultures were serial diluted and spotted onto LB plates supplemented or not with deoxycholate 2%. After overnight incubation at 37 °C, survival was reported as the highest dilution of strain able to form colonies.

Colicin susceptibility. Colicin activities were tested as described (18). Briefly, over-night cultures of the strains were spread on LB agar petri dishes supplemented with antibiotics. Plasmid expression was induced using L-arabinose (0.02%) and IPTG (100 µM). After drying, 1 µL of serial dilutions (10 fold) of colicin A and colicin B were spotted on the bacterial lawn. Plates were incubated at 37°C for 16 hrs.

fd-Tc phage preparation and titration. fd-Tc phages were produced from an infected *E. coli* GM1 strain as described otherwhere (18) with the following modifications. After 16 hrs of culture, the cells were pelleted by two rounds of centrifugation at 5,000 g for 20 min. Phages were isolated from the supernatant using the isoelectric precipitation method (Mourez *et al*, 2004). Briefly, the phage suspension was brought to pH=4.6 with HCl and centrifuged at 13,000 g for 20 min in order to precipitate the particles. The phage pellet was rinsed with deionized water, centrifuged again at 13,000g for 10 min, and the phages were finally resuspended in PBS buffer 1X pH 7.0 and filter-sterilized (0.45 µm syringe filter). Phage preparations were checked for sterility by plating on LB plate. Titration of the WT phage suspension was performed using standard protocols (18). To calculate the number of mutant phage particles in each samples, absorbance readings were taken at 269 nm and 320 nm using a Carry-UV spectrophotometer (Agilent). The titer was calculated using the following formula (Abs. 269 - Abs. 320) × 6 × 1016/plasmid size, with 9183 nt for the fd-Tc genome (Mourez *et al*, 2004).

Susceptibility to fd-Tc phage infection assays. Strains of interest were cultivated to reach OD600nm =0.7 to 0.8 and normalized to the same initial OD600nm. For F+ infection, 10 µl of phage suspension was added to 200 µL GM1 F+ cells (multiplicity of infection of 1,000 phages per bacteria). Infection assay were performed in triplicate in 96-well plates, during 30 min of incubation at room temperature without shaking. The cells were vigorously homogenized by pipetting, and immediately serial diluted 10 fold in sterile PBS. 5 µl were drops on a LB plate (total recipient CFU) or LB agar supplemented with Tc (15 ng/µl) (phage infected CFU).

For F-independent infection, 450 µL of W3110 cells were treated with 10 µM CCCP for 3 min at room temperature. Cells were centrifuged 5 min at 8,000 rpm and the pellet was resuspended in 50 µL CaCl2 50 mM and incubated for 15min with 25 µL of phage suspension. The cells were submitted to vigorous vortexing and two rounds of centrifugation and wash in 700 µL sterile PBS in order to remove unattached and reversibly attached phages. Finally, the pellet was resuspended in 60 µL LB and incubated for 10 min at 37°C for recovery before serial dilution and spreading on LB or LB+Tc plates. After overnight incubation at 37°C, isolated CFU were counted in the appropriate dilution test. The frequency of infection (F) was determined by dividing the number of infected cells by the number of total recipient cells. Experiments were conducted in triplicates.

Phage stability assay by agarose gel electrophoresis. Virions samples were fully disassembled by incubation in 1% SDS-supplemented DNA loading dye (1X Tris–acetate–EDTA (TAE) buffer, 5% glycerol, 0.25% bromophenol blue pH 8.3) at 70 °C for 15 min. For stability assays, virions were mixed with 0.1% Sarkosyl-supplemented loading dye and incubated at room temperature for 10 min prior to electrophoresis. Samples were loaded onto TAE 1X agarose gels (0.6%). Electrophoresis were performed at 50V for two hours. The ssDNA released from the phage particles was visualized by staining the gel with Gelred dye for 45 min.

Supporting bibliography

Battesti, A., and Bouveret, E. (2008) Improvement of bacterial two-hybrid vectors for detection of fusion proteins and transfer to pBAD-tandem affinity purification, calmodulin binding peptide, or 6-histidine tag vectors. Proteomics. 8, 4768–4771

Houot, L., Navarro, R., Nouailler, M., Duché, D., Guerlesquin, F., and Lloubes, R. (2017) Electrostatic interactions between the CTX phage minor coat protein and the bacterial host receptor TolA drive the pathogenic conversion of Vibrio cholerae. Journal of Biological Chemistry. 292, 13584–13598

Karimova, G., Pidoux, J., Ullmann, A., and Ladant, D. (1998) A bacterial two-hybrid system based on a reconstituted signal transduction pathway. Proc. Natl. Acad. Sci. U.S.A. 95, 5752–5756

Mourez, M., and Collier, R. J. (2004) Use of Phage Display and Polyvalency to Design Inhibitors of Protein–Protein Interactions. in Protein-Protein Interactions, pp. 213–228, Humana Press, New Jersey, 261, 213–228

Vieira, J., and Messing, J. (1991) New pUC-derived cloning vectors with different selectable markers and DNA replication origins. Gene. 100, 189–194

Samire, P., Serrano, B., Duché, D., Lemarié, E., Lloubès, R., and Houot, L. (2020) Decoupling Filamentous Phage Uptake and Energy of the TolQRA Motor in Escherichia coli. J Bacteriol. 10.1128/JB.00428-19

Zhang, X. Y.-Z., Goemaere, E. L., Thomé, R., Gavioli, M., Cascales, E., and Lloubés, R. (2009) Mapping the Interactions between Escherichia coli Tol Subunits. Journal of Biological Chemistry. 284, 4275–4282

Zhang, X. Y.-Z., Goemaere, E. L., Seddiki, N., Célia, H., Gavioli, M., Cascales, E., and Lloubes, R. (2011) Mapping the Interactions between Escherichia coli TolQ Transmembrane Segments. Journal of Biological Chemistry. 286, 11756–11764